

Product Centered Dirichlet Processes for Bayesian Multiview Clustering

Alexander Dombowsky¹ and David B. Dunson^{1,2}

¹Department of Statistical Science, Duke University, Durham, NC, USA

²Department of Mathematics, Duke University, Durham, NC, USA

Abstract

While there is an immense literature on Bayesian methods for clustering, the multiview case has received little attention. This problem focuses on obtaining distinct but statistically dependent clusterings in a common set of entities for different data types. For example, clustering patients into subgroups with subgroup membership varying according to the domain of the patient variables. A challenge is how to model the across-view dependence between the partitions of patients into subgroups. The complexities of the partition space make standard methods to model dependence, such as correlation, infeasible. In this article, we propose CLustering with Independence Centering (CLIC), a clustering prior that uses a single parameter to explicitly model dependence between clusterings across views. CLIC is induced by the product centered Dirichlet process (PCDP), a novel hierarchical prior that bridges between independent and equivalent partitions. We show appealing theoretic properties, provide a finite approximation and prove its accuracy, present a marginal Gibbs sampler for posterior computation, and derive closed form expressions for the marginal and joint partition distributions for the CLIC model. On synthetic data and in an application to epidemiology, CLIC accurately characterizes view-specific partitions while providing inference on the dependence level.

Keywords: Bayesian inference; multiview clustering; random partitions; mixture models; Bayesian nonparametrics

1 INTRODUCTION

Many application areas collect *multiview* data comprising several different types of information on the same set of objects. Multiomics data, for example, consist of various molecular features, such as single nucleotide polymorphisms (SNPs), RNA expression, and DNA methylation measured on the same

arXiv:2312.05365v3 [stat.ME] 3 Oct 2024

sample (Rappoport and Shamir, 2018). The particular focus of this article is on *multiview clustering*, a field which generalizes standard cluster analysis to multiview data; see Bickel and Scheffer (2004) and Fang et al. (2023) for an overview of the developments in this area. For example, it is broadly of interest to infer patient subgroups based on three views: molecular biomarkers, clinical covariates, and disease outcomes. These views may be of vastly different dimension or type. Often, the biomarkers measure counts for tens of thousands of genes, the covariates consist of categorical demographic information and numeric laboratory results, and the disease outcomes are a single binary variable indicating mortality. Multiview clustering methods seek to incorporate or balance these markedly different attributes when inferring the subgroups.

Previously, the term multiview clustering referred to a technique in which contributions from the different views are incorporated into a single integrative clustering. However, more recent approaches have expanded the notion of multiview clustering to address the aim of *multiple clustering* (Yao et al., 2019; Wei et al., 2020; Franzolini et al., 2023), a related field which derives multiple clusterings for a single dataset (Yu et al., 2024). While the input for a multiple clustering algorithm need not be multiview, the clusterings generated by said algorithm are created to be as dissimilar as possible to reflect different perspectives of the data (Bailey, 2014). In this article, we refer to multiview clustering as the problem of inferring separate but statistically dependent groupings in the same objects for the different views under consideration. Returning to our earlier example, this framework entails inferring three groupings of the hospital patients: one informed by the molecular biomarkers, another based on clinical characteristics, and a third reflecting differences in the conditional distribution of the outcomes given the biomarkers and covariates.

There are several practical reasons why multiview clustering is preferable to applying a clustering algorithm to a single, consolidated feature set. A key benefit of multiview clustering is interpretability of the results; the clustering associated with a certain view reflects the variation within that view. Next, the multiview approach ensures that some views do not become obscured in the clustering procedure by other views of higher dimension. In the case where one view is a low dimensional outcome and the other is a set of covariates, the posterior distribution under a single partition is dominated by the likelihood of the predictors, obscuring any grouping structure indicated by the dependent variable (Wade et al., 2014). Even in low dimensional settings, clustering algorithms are skewed towards capturing variability in the views with higher dimension (Franzolini et al., 2023).

Finally, investigators are often interested in the relationship between the clusterings, e.g., assessing whether covariate subgroups map well to patterns in the outcome.

The Bayesian framework is appealing for multiview clustering due to its ability to model complex dependence structures and quantify clustering uncertainty. However, Bayesian methodology was seldom applied to multiview clustering analyses until relatively recently, and earlier models focused on capturing a specific notion of dependence rather than defining a general measure of clustering correlation. Bayesian consensus clustering (Lock and Dunson, 2013; Lu and Lou, 2022) induces across view dependence by a latent integrative clustering of the objects and is primarily motivated by multiomics data. The integrative clustering is not just a vessel to imbue dependence, but moreso a primary focus of inference in order to obtain a single unified grouping of the observations. In general, we may not want to assume that such an integrative clustering exists. Alternatively, enrichment (Wade et al., 2011, 2014) addresses prediction with clustering models, and enforces dependence by requiring that the clusters in the outcome be subsets of the clusters in the covariates. Nested clustering models have also been utilized by Lee et al. (2016) and Franzolini et al. (2023). The nested assumption can be rather rigid in practice, as clusterings can still be similar without having a tree structure.

We focus on inducing a broader sense of cluster dependence. Generally, there are two extremes for specifying a probabilistic clustering model for multiview data. On one end of the spectrum is the single partition model, which arises when all view-specific partitions are equivalent. In this case, the relationship between the partitions is trivially dependent. Conversely, assuming that there are independent partitions associated with each view fails to acknowledge the possibility of across-view dependence induced by clustering the same set of objects. If two objects are co-clustered together under one view, we would like to incorporate this information when deciding whether to co-cluster them under another.

In this paper, we propose a framework for modeling dependent partitions with a single parameter controlling dependence, bridging between identical partitions for the different views and independence at the two extremes. Let \mathcal{P}_n be the set partitions of the integers $[n] = \{1, \dots, n\}$ and suppose we randomly draw two partitions $C_1, C_2 \in \mathcal{P}_n$, where $C_v = (C_{v1}, \dots, C_{vK_v})$. Alternatively, we may express the partitions as n -dimensional labelings $\mathbf{c}_v = (c_{v1}, \dots, c_{vn})$ with $c_{vi} \in [K_v] = \{1, \dots, K_v\}$ for all $i = 1, \dots, n$. C_1 and C_2 represent partitions of the same data for different views. The *Rand index* (Rand, 1971) between C_1 and C_2 is defined as $R(C_1, C_2) = \{A_{12} + B_{12}\} / \binom{n}{2}$, where $A_{12} = \sum_{i < j} \mathbf{1}_{c_{1i}=c_{1j}, c_{2i}=c_{2j}}$ and $B_{12} = \sum_{i < j} \mathbf{1}_{c_{1i} \neq c_{1j}, c_{2i} \neq c_{2j}}$ count the number of shared pairwise clus-

tering decisions. If C_1 and C_2 are equivalent, $R(C_1, C_2) = 1$. Assuming that π is a joint distribution with support on \mathcal{P}_n , we will be interested in the expected Rand index (ERI) $\tau_{12} := \mathbb{E}[R(C_1, C_2)] = \sum_{C_1, C_2 \in \mathcal{P}_n} R(C_1, C_2) \pi(C_1, C_2)$. If $C_1 \perp C_2$ a priori, i.e. $\pi(C_1, C_2) = \pi(C_1)\pi(C_2)$, we denote the resulting ERI as $\tau_{12}^0 = \sum_{C_1, C_2 \in \mathcal{P}_n} R(C_1, C_2) \pi(C_1)\pi(C_2)$. The form of τ_{12}^0 depends on the hyperparameters of the marginal probability mass functions (PMFs) $\pi(C_1)$ and $\pi(C_2)$. We introduce CLustering with Independence Centring (CLIC), a class of joint distributions on \mathcal{P}_n with the property that for some $\rho > 0$,

$$\tau_{12} = \frac{1}{\rho + 1} + \left(1 - \frac{1}{\rho + 1}\right) \tau_{12}^0. \quad (1)$$

That is, the ERI is a weighted average between 1, the ERI of two equivalent random partitions, and τ_{12}^0 , the ERI of two independent random partitions. Notice that ρ controls concentration towards the independent clustering model. In practice, one is uncertain about ρ , but we will show that a conjugate prior naturally arises under a specific data augmentation scheme. This will allow one to infer the posterior distributions of both (C_1, C_2) and ρ .

Our model is induced by altering the Dirichlet process (DP) prior (Ferguson, 1973) for generating random measures with support on some space Θ . The DP is parameterized with a *concentration parameter* $\gamma > 0$, and a *base measure* H on Θ . Let S_1, \dots, S_K be any partition of Θ , i.e. $S_k \cap S_l = \emptyset$ and $\bigcup_{k=1}^K S_k = \Theta$. We say that $P \sim \text{DP}(\gamma, H)$ if $(P(S_1), \dots, P(S_K)) \sim \text{Dir}(\gamma H(S_1), \dots, \gamma H(S_K))$. The elementary properties of the Dirichlet distribution imply that H can be viewed as the center of the DP with variation controlled by γ . The larger γ is, the more concentrated the prior on P is at the base measure H .

Sethuraman (1994) showed that realizations from the Dirichlet process are almost surely discrete even if H is non-atomic. For that reason, a sample $\theta_1, \dots, \theta_n \sim P$ is expected to have a number of repeated values. By grouping objects with the same value of θ_i , we create index sets known as *clusters*, ultimately inducing a partition $C = (C_1, \dots, C_K) \in \mathcal{P}_n$. If we marginalize out the DP prior on P , the induced prior on C is the Chinese Restaurant Process (CRP) (Aldous, 1985). $C \sim \text{CRP}(\gamma)$ if its PMF is

$$\pi^{\text{CRP}}(C \mid \gamma) = \frac{\gamma^K}{\prod_{i=1}^n (\gamma + i - 1)} \prod_{k=1}^K (n_k - 1)!, \quad (2)$$

where $n_k = |C_k|$ is the size of the k th cluster for $k = 1, \dots, K$. The number of clusters in the CRP is governed by γ , and one can show that $\mathbb{E}(K)/\log n \rightarrow \gamma$ as $n \rightarrow \infty$. The clustering properties of

the DP prior are particularly useful in Dirichlet Process Mixtures (DPMs) in which θ_i determines the distribution of data for object i (Antoniak, 1974).

We return now to our original aim of modeling dependent partitions. Suppose that $\Theta = \Theta_1 \times \Theta_2$ for some parameter spaces Θ_v for $v = 1, 2$. Here, the index v corresponds to the view of the data, whether it be multiomics or covariates and an outcome. To induce two view-specific partitions of $[n]$, we decompose the atoms into $\theta_i = (\theta_{1i}, \theta_{2i})$, where $\theta_{vi} \in \Theta_v$. We define the product centered Dirichlet process (PCDP) to be the following prior for a random measure P on Θ ,

$$\begin{aligned} P \mid \rho, Q_1, Q_2 &\sim \text{DP}(\rho, Q_1 \times Q_2); \\ Q_v \mid \gamma_v, H_v &\sim \text{DP}(\gamma_v, H_v) \text{ for } v = 1, 2; \end{aligned} \tag{3}$$

where $\gamma_v > 0$ and H_v has support on Θ_v , and \times denotes the product measure. By counting ties in θ_{1i} and θ_{2i} , the PCDP creates two dependent partitions $C_1, C_2 \in \mathcal{P}_n$ with ERI given by (1) and $\tau_{12}^0 = \sum_{C_1, C_2 \in \mathcal{P}_n} R(C_1, C_2) \pi^{\text{CRP}}(C_1 \mid \gamma_1) \pi^{\text{CRP}}(C_2 \mid \gamma_2)$. The induced joint partition distribution is denoted by $(C_1, C_2) \sim \text{CLIC}(\rho, \gamma_1, \gamma_2)$. We will show that increasing values of ρ will result in independent $\text{CRP}(\gamma_v)$ partitions, whereas increasing values of γ_v results in two identical $\text{CRP}(\rho)$ partitions.

The PCDP is related to but distinct from methods for Bayesian nonparametric modeling of data from subjects in different groups, including the hierarchical Dirichlet process (HDP) (Teh et al., 2006; Ren et al., 2008; Paisley et al., 2014) and the nested Dirichlet process (NDP) (Rodriguez et al., 2008). In this literature, groups are prespecified and contain different subjects, and the focus is on borrowing of information in inferring group-specific distributions while clustering the subjects in different groups. Particularly relevant is the HDP, which models a random measure for each group using a hierarchical DP prior in which the base measure Q is itself modeled as a DP. Conversely, (3) simulates a single random probability distribution whose base measure is a product of DP distributed measures. The goal of the PCDP is fundamentally different in inducing dependence across views in clustering a single set of subjects. However, the marginal distributions of measures drawn from a PCDP will be HDPs, and the Gibbs sampler for the HDP will be useful for inferring the posterior of our induced CLIC model. More generally, the PCDP is not an example of a hierarchical process (Camerlenghi et al., 2018, 2019), but theoretical tools established by the literature on hierarchical processes will be essential for deriving the closed form expression of the $\text{CLIC}(\rho, \gamma_1, \gamma_2)$ probability mass function.

The PCDP and CLIC contribute to an emerging literature on Bayesian inference for dependent clustering models. Besides nested clusterings such as the enriched Dirichlet process, temporally correlated partitions have been modeled using a generalized Pólya urn scheme in [Caron et al. \(2007\)](#) and [Caron et al. \(2017\)](#), and a sequence of cluster re-allocations in [Page et al. \(2022\)](#). The latter approach exhibits a similar ERI to (1) when $n = 2$. An approximate Bayes approach for multiview clustering was proposed in [Duan \(2020\)](#) that models the similarity matrix of each view as a noisy realization from a cluster graph. [Franzolini et al. \(2023\)](#) introduced conditional partial exchangeability (CPE), a general framework for modeling dependent partitions that encompasses the models of [Wade et al. \(2011\)](#), [Lee et al. \(2016\)](#), and [Page et al. \(2022\)](#). A two view clustering model satisfies CPE if the data are exchangeable conditional on C_1 and C_2 , and, additionally, the data in the second view are partially exchangeable conditional on C_1 . CLIC satisfies these CPE assumptions under certain settings. Furthermore, the CLIC parameter ρ in (1) is a transformation of the expected telescopic adjusted Rand index (TARI), a measure of clustering dependence proposed by [Franzolini et al. \(2023\)](#). In contrast to their methods, CLIC directly models uncertainty in clustering dependence by assigning ρ a prior, does not assume a directional relationship between C_1 and C_2 , and induces a different joint partition probability function for (C_1, C_2) .

This paper is organized as follows. In Section 2 we propose the PCDP as a model for dependent random measures, show basic theoretic properties, and derive a finite approximation that is analogous to other random measure priors ([Ishwaran and Zarepour, 2002](#); [Lijoi et al., 2023](#)). In Section 3, we focus on CLIC, the induced dependent partition distribution of the PCDP. We prove that (1) holds for the $\text{CLIC}(\rho, \gamma_1, \gamma_2)$ distribution and derive the closed form expression for its PMF, which we call a marginally exchangeable partition probability function (MEPPF). A marginal Gibbs sampler for the finite approximation is discussed in Section 4. We evaluate CLIC as a clustering method for synthetic multiview data in Section 5 and in an application to the Collaborative Perinatal Project (CPP) in Section 6. Finally, we provide concluding remarks and extensions in Section 7.

2 PRODUCT CENTERED DIRICHLET PROCESSES

2.1 MULTIVIEW CLUSTERING

We assume that the data are split into two views $\mathbf{X} = (\mathbf{X}_1, \mathbf{X}_2)$, where $\mathbf{X}_v = (X_{v1}, \dots, X_{vn})$ and $X_{vi} \in \Omega_v$ for $v = 1, 2$, though our methodology can be generalized to more than two views. The

views may be of varying dimension and data type. For instance, the views could be different omics measurements or an outcome and covariates. The dimension of each view is denoted by d_v for all $v = 1, \dots, V$, and the variables in the v th view are indicated with the index j_v . Associated with the i th observation is parameter $\theta_i = (\theta_{1i}, \theta_{2i}) \in \Theta = \Theta_1 \times \Theta_2$ for view-specific parameter spaces Θ_1, Θ_2 . We model the data using a multiview mixture model in which θ_i determines the probability distribution of $X_i = (X_{1i}, X_{2i})$. That is,

$$X_i | \theta_i \sim f(X_i; \theta_i), \quad \theta_i | P \sim P, \quad \text{for } i = 1, \dots, n; \quad (4)$$

where $f(\cdot; \theta)$ is a parametric probability distribution that depends on θ and P is a probability distribution with support on Θ , often called the mixing measure. We will assume that P is almost surely discrete, so that draws $\theta_1, \dots, \theta_n \sim P$ are guaranteed to have unique values $\theta_1^*, \dots, \theta_K^*$ for some $K < \infty$. Additionally, there will be ties within each view represented by the unique values $\theta_{v1}^*, \dots, \theta_{vK_v}^*$.

We create *clusters* by grouping observations with identical atoms. Let $C_{vk_v} = \{i : \theta_{vi} = \theta_{vk_v}^*\}$ be the k_v th cluster in the v th view. The view-specific partitions are defined as $C_v = (C_{v1}, \dots, C_{vK_v})$ with associated labelings similarly defined as $\mathbf{c}_v = (c_{v1}, \dots, c_{vK_v})$, where $c_{vi} = k_v \iff i \in C_{vk_v}$. The size of C_{vk_v} is denoted by $n_{vk_v} = |C_{vk_v}|$, which we collect into the vector $\mathbf{n}_v = (n_{v1}, \dots, n_{vK_v})$. While we consider ties in θ_{i1} and θ_{i2} separately, we will also observe ties in θ_i , i.e. $\theta_i = \theta_j \iff \theta_{i1} = \theta_{j1}$ and $\theta_{i2} = \theta_{j2}$. These ties are represented by a *cross-partition* or *cross-clustering* $D = (D_{k_1k_2})_{k_1, k_2}$, where $D_{k_1k_2} = C_{1k_1} \cap C_{2k_2}$ for $k_1 = 1, \dots, K_1$ and $k_2 = 1, \dots, K_2$. The cross-partition is an object describing the joint distribution of two random partitions, analogous to collecting random variables into a random vector. The cross-clustering is related to the *contingency table* between C_1 and C_2 , given by $\mathbf{n} = (n_{k_1k_2})_{k_1, k_2}$ where $n_{k_1k_2} = |D_{k_1k_2}|$. The contingency table can be reverted to the cluster sizes using summations, i.e. $n_{1k_1} = \sum_{k_2} n_{k_1k_2}$ and $n_{2k_2} = \sum_{k_1} n_{k_1k_2}$. As we will discuss later on, \mathbf{n} will be crucial for interpretation and computation of our model.

Observe that we can rewrite the distribution of X_i in (4) as $(X_i | c_{1i} = k_1, c_{2i} = k_2, \theta_{1k_1}^*, \theta_{2k_2}^*) \sim f(X_i; \theta_{1k_1}^*, \theta_{2k_2}^*)$. We address two cases in which dependent clustering may arise. The first is when the views are assumed to be independent conditional on the clusterings,

$$X_i | c_{1i} = k_1, c_{2i} = k_2, \theta_{1k_1}^*, \theta_{2k_2}^* \sim f_1(X_{1i}; \theta_{1k_1}^*) \times f_2(X_{2i}; \theta_{2k_2}^*), \quad (5)$$

where $f_v(\cdot; \theta_v)$ is a parametric probability distribution for the v th view. Here, we can interpret C_1 as a clustering for \mathbf{X}_1 and C_2 as a clustering for \mathbf{X}_2 . In the case of multiomics, C_1 may be a partition related to SNPs, whereas C_2 represents a partition induced by RNA expression. The kernel in (5) is equivalent to assuming that the relationship between C_1 and C_2 comprises the overall across view dependence structure. If, for example, C_1 and C_2 are independent, then $X_{1i} \perp X_{2i}$.

Conversely, for covariate-outcome data, it may be more appropriate to model the data with

$$X_i \mid c_{1i} = k_1, c_{2i} = k_2, \theta_{1k_1}^*, \theta_{2k_2}^* \sim f_1(X_{1i}; \theta_{1k_1}^*) \times f_2(X_{2i}; X_{1i}, \theta_{2k_2}^*), \quad (6)$$

where $f_2(\cdot; \cdot, \theta_2)$ is a parametric conditional distribution and $f_1(\cdot; \theta_1)$ is the marginal distribution for \mathbf{X}_1 . We then interpret C_1 as \mathbf{X}_1 clusters, but C_2 are now $(\mathbf{X}_2 \mid \mathbf{X}_1)$ clusters, i.e. clusters related to the conditional distribution of the second view given the first. For example, if $X_{i1}, X_{2i} \in \mathbb{R}$, (6) can be modeled with a linear regression model $f_2(X_{2i}; X_{1i}, \theta_{2k_2}^*) = \mathcal{N}(X_{2i}; X_{1i}\theta_{2k_2}^*, \sigma^2)$. C_2 groups together observations with a similar relationship between the covariates \mathbf{X}_1 and the response \mathbf{X}_2 . If $C_1 \perp C_2$, then groups based off the covariates are not useful for prediction. Observe that if there are V sub-views amongst the covariates \mathbf{X}_1 , we can model $f_1(X_{1i}; \theta_{1k_1}^*)$ with the product kernel in (5), resulting in $V + 1$ dependent partitions comprising the outcome and the covariate sub-views.

The main motivation of this article is to address the dependence structure between C_1 and C_2 . On one end of the spectrum, $C_1 \perp C_2$, meaning that the clustering of one view gives no information about the clustering in the other. There are a wide variety of methods to model independent clusterings for (5) and (6) using random measures, such as setting $P = P_1 \times P_2$, where $P_1 \perp P_2$ and each P_v follows a DP prior. On the other hand, the two clusterings could be trivially dependent, i.e. $C_1 = C_2$ almost surely. Trivially dependent clusterings imply that the underlying grouping structure of \mathbf{X} is unchanged between the views. If $C_1 = C_2$, one can see that \mathbf{n} is a generalized permutation matrix, i.e. there is only one non-zero entry in each row and column of the contingency table. This clustering model can be implemented by assuming P is drawn from a DP prior with a non-atomic base measure, as ties in θ_{1i} are equivalent to ties in θ_{2i} . We are interested in defining a model bridging between independent and identical clusterings across the views, allowing nontrivial dependence between C_1 and C_2 .

2.2 PRIOR ON THE MIXING MEASURE

The product centered Dirichlet process (PCDP) is a nonparametric prior for random measures that can model dependence between partitions. To begin, we assume that the parameter space is a Cartesian product of view-specific parameter spaces, i.e. $\Theta = \Theta_1 \times \Theta_2 = \{(\theta_{1k_1}^*, \theta_{2k_2}^*) : \theta_{vk_v}^* \in \Theta_v\}$. At the top level, we draw P from a DP conditional on a concentration parameter ρ and a base measure Q ,

$$P \mid \rho, Q \sim \text{DP}(\rho, Q). \quad (7)$$

Since P is drawn from a DP, it is guaranteed to be almost surely discrete (Sethuraman, 1994), which ultimately leads to clusters in the data generating process. This procedure can be better visualized with the Pólya urn scheme (Blackwell and MacQueen, 1973), which computes the conditional distribution of the i th atom after marginalizing out P :

$$\theta_i \mid \theta_1, \dots, \theta_{i-1}, \rho, Q \sim \sum_{j=1}^{i-1} \left(\frac{1}{\rho + i - 1} \right) \delta_{\theta_j} + \frac{\rho}{\rho + i - 1} Q, \quad (8)$$

where δ_{θ_j} is the degenerate measure at θ_j . With probability $1/(\rho + i - 1)$, we set θ_i equal to one of the already generated atoms θ_j , placing i into an already created cluster. Otherwise, with probability $\rho/(\rho + i - 1)$, we simulate $\theta_i \sim Q$, generating a potentially new value.

Observe that Q must be carefully chosen in order to induce non-trivially dependent clusters. Suppose that Q is some non-atomic distribution, i.e. $Q(\{(\theta_{1k_1}^*, \theta_{1k_2}^*)\}) = 0$ for any pair of atoms. Under this regime, (8) implies that $C_1 = C_2$ almost surely since $\theta_{1i} = \theta_{1j} \iff \theta_{2i} = \theta_{2j}$. When dealing with the standard DP and non-atomic base measure, there are only two choices when sampling the i th atom in (8): sample θ_i from an existing cluster or create a new cluster. This scheme is visualized using the Chinese restaurant process (CRP) metaphor. Here, θ_i are customers entering a Chinese restaurant with an infinite amount of tables. They can either sit at one of the occupied tables, indicated by $\theta_i = \theta_j$, or sit at an unoccupied table, which corresponds to sampling $\theta_i \sim Q$ (Aldous, 1985). In contrast, the cross-clustering case motivates four choices: set θ_{1i} and θ_{2i} equal to existing atomic values, set $\theta_{1i} = \theta_{1j}$ and generate a new value of θ_{2i} , set $\theta_{2i} = \theta_{2j}$ and generate a new value of θ_{1i} , or generate two new values of θ_{1i} and θ_{2i} . In a dependent clustering model, each of these possibilities should have positive probability when simulating θ_i . Alternatively, if we were to simulate

$\theta_{1i} \sim P_1$ and $\theta_{2i} \sim P_2$, where $P_v \sim \text{DP}(\rho_v, Q_v)$ independently, then there would indeed be the desired four choices when sampling θ_i , but $C_1 \perp C_2$.

A middle ground between the independent and trivially dependent case is induced by assigning Q an appropriate prior distribution. The first step is to construct Q using marginals on Θ_v . Let Q_v be probability distributions on $(\Theta_v, \mathcal{S}_v)$, where \mathcal{S}_v is a σ -algebra on Θ_v , for $v = 1, 2$. The product measure $Q = Q_1 \times Q_2$ is defined by $Q(S_1 \times S_2) = Q_1(S_1)Q_2(S_2)$ for any $S_1 \in \mathcal{S}_1$ and $S_2 \in \mathcal{S}_2$. Occasionally, the notation $Q = \times_{v=1}^2 Q_v$ may be used to refer to the product measure. We will furthermore assume that Q_v are also drawn from DP priors, i.e.

$$Q_v \mid \gamma_v, H_v \sim \text{DP}(\gamma_v, H_v) \text{ independently for } v = 1, 2. \quad (9)$$

We will typically take H_v to be non-atomic. Since Q_v are themselves probability measures, Q is guaranteed to exist and be unique almost surely (Resnick, 2001), and its marginal distributions are Q_1 and Q_2 . Observe that if $\rho \rightarrow \infty$, then $P = Q$ and, therefore, $C_1 \perp C_2$. For this reason, we interpret Q as the null case, with degree of concentration controlled by ρ , and call (7) and (9) the PCDP for modeling random measures. Observe that there are three concentration parameters in this process: γ_1 , γ_2 , and ρ . In the Supplemental Material, we verify that these hyperparameters are identifiable for $\pi(P, Q_1, Q_2 \mid \rho, \gamma_1, \gamma_2)$ for any non-atomic base measures H_1 and H_2 . In practice, we fix γ_1 and γ_2 , but a similar argument implies identifiability for ρ in this case.

This formulation is distinct from the HDP (Teh et al., 2006), which assumes that P follows (7) and $Q \sim \text{DP}(\gamma, H)$, with no specification on the marginals. One can show that when Q_1 and Q_2 follow (9), their product measure is not distributed as a DP. For example, let $S_v \in \mathcal{S}_v$ for $v = 1, 2$. Then we construct a partition of Θ using the sets $S_1 \times S_2$, $S_1 \times S_2^c$, $S_1^c \times S_2$, and $S_1^c \times S_2^c$, where $S_v^c = \Theta_v \setminus S_v$. We then have, for instance, that $Q(S_1 \times S_2) = Q_1(S_1)Q_2(S_2)$, where $Q_v(S_v) \sim \text{Beta}(\gamma_v H_v(S_v), \gamma_v H_v(S_v^c))$ for $v = 1, 2$ and are independent. Hence, $Q(S_1 \times S_2)$ is not distributed as a Beta random variable and instead follows a Wilks' type-B distribution (Wilks, 1932; Tang and Gupta, 1984). On the other hand, the marginals of P will be distributed as HDPs. Define $P_1(\cdot) = \int_{\Theta_2} dP(\cdot, \theta_2)$ and $P_2(\cdot) = \int_{\Theta_1} dP(\theta_1, \cdot)$, to be the marginal distributions of P on Θ_v for $v = 1, 2$. For example, conditional on Q_1, Q_2 and

given the partition S_{11}, \dots, S_{1m} of Θ_1 , Fubini's theorem implies

$$\begin{aligned} (P_1(S_{11}), \dots, P_1(S_{1m})) &\stackrel{d}{=} (P(S_{11} \times \Theta_2), \dots, P(S_{1m} \times \Theta_2)) \\ &\sim \text{Dir}(\rho Q_1(S_{11}), \dots, \rho Q_1(S_{1m})), \end{aligned} \quad (10)$$

and a similar property holds for P_2 . In other words, the prior for the marginals is $P_v \mid \rho, Q_v \sim \text{DP}(\rho, Q_v)$, $Q_v \sim \text{DP}(\gamma_v, H_v)$.

Using (8) and (9), we can express a Pólya urn scheme for the PCDP. For observation i , we observe $K^{(i)} \leq i - 1$ unique values in $\theta^{(i)} = (\theta_1, \dots, \theta_{i-1})$ since P is almost surely discrete. Across the views, this translates into unique atoms $\theta_{v1}^*, \dots, \theta_{vK_v^{(i)}}^*$, where $K_v^{(i)} \leq K^{(i)}$ for $v = 1, 2$. In order to compute the predictive distribution of θ_i , we must marginalize out Q from (8). Since Q is almost surely discrete and a product measure, we derive a unique form of the usual Pólya urn scheme for Bayesian clustering.

Theorem 1. The distribution of the i th atom conditional on the first $i - 1$ atoms is

$$\theta_i \mid \theta^{(i)}, \rho \sim \sum_{k_1, k_2} \frac{n_{k_1 k_2}}{\rho + i - 1} \delta_{(\theta_{1k_1}^*, \theta_{2k_2}^*)} + \frac{\rho}{\rho + i - 1} \times_{v=1}^2 \left\{ \sum_{k_v=1}^{K_v^{(i)}} \frac{r_{vk_v} \delta_{\theta_{vk_v}^*}}{\gamma_v + r^{(i)}} + \frac{\gamma_v H_v}{\gamma_v + r^{(i)}} \right\}, \quad (11)$$

where $\mathbf{r}_v = (r_{v1}, \dots, r_{vK_v^{(i)}})$, $r_{vk_v} \in \{0, \dots, n_{vk_v}\}$, and $\sum_{v=1}^{K_v^{(i)}} r_{vK_v} = r^{(i)}$ for $v = 1, 2$.

The two terms in (11) can be interpreted in terms of an independence centered CRP metaphor. Suppose that θ_{1i} denotes the table and θ_{2i} denotes the entrée of the i th customer. With probability $1/(\rho + i - 1)$, the customer sits at an occupied table and, seeing an appetizing dish already placed at the table, orders the same entrée as one of their tablemates, which is indicated by setting $\theta_i = \theta_j$. The probability of each option is weighted by their corresponding entry in the contingency table, so popular combinations of table and entrée will have more of an influence on customer i 's choice. Otherwise, with probability $\rho/(\rho + i - 1)$, the customer chooses a table and orders an entrée independently. By the time customer i has entered the restaurant, $r^{(i)} \leq i - 1$ customers have made their table and entrée choices independently. Of these $r^{(i)}$ people, r_{1k_1} have sat down at table k_1 and r_{2k_2} have ordered entrée k_2 . The vector \mathbf{r}_1 is just the number of customers at each table who made their choices independently, and \mathbf{r}_2 is the same but across the entrées. If customer i 's choice of table and entrée are independent, then the probability of sitting at table k_1 is weighted by r_{1k_1} , and a similar property holds for the entrée with r_{2k_2} .

We can then update (11) for customer $i + 1$ by adhering to the following rules. If customer i selects table k_1 and entrée k_2 from the contingency table \mathbf{n} , we set $n_{k_1 k_2} = n_{k_1 k_2} + 1$. Otherwise, customer i chooses independently and we set $r^{(i+1)} = r^{(i)} + 1$. If customer i happens to choose table k_1 and entrée k_2 , we set $n_{k_1 k_2} = n_{k_1 k_2} + 1$, $r_{1k_1} = r_{1k_1} + 1$, and $r_{2k_2} = r_{2k_2} + 1$. Suppose now that, given customer i chooses independently, they opt for table k_1 but order a new entrée. Then we would create a new entry $n_{k_1(K_2^{(i)}+1)} = 1$ in the contingency table, create a new entry of \mathbf{r}_2 given by $r_{2(K_2^{(i)}+1)} = 1$, and set $r_{1k_1} = r_{1k_1} + 1$. A similar rule holds for sitting at a new table but asking for an already ordered entrée. Finally, if customer i opts for both a new table and new entrée, we create $n_{(K_1^{(i)}+1)(K_2^{(i)}+1)} = 1$, $r_{1(K_1^{(i)}+1)} = 1$, and $r_{2(K_2^{(i)}+1)} = 1$.

Clearly, the larger ρ is, the less likely it is that the choice of table depends on the choice of entrée, meaning that all dishes should be distributed independently across the restaurant, $r^{(i)} \rightarrow i - 1$, and $\mathbf{r}_v \rightarrow \mathbf{n}_v$ for $v = 1, 2$. However, the marginal concentration parameters γ_v will have an impact on these choices as well. If, instead, we took $\gamma_1, \gamma_2 \rightarrow \infty$, we will find the opposite: all the customers at each table will order the same entrée, and no two tables will have the same dish. That is, the choice of food is equivalent to the choice of a table. This behavior can be seen by taking limits in (11), but we can also state these limiting properties in terms of P .

Proposition 1. Recall that \mathcal{S}_v is a σ -algebra on Θ_v for $v = 1, 2$.

1. Fix γ_1, γ_2 and let $S \subset \Theta$. Then as $\rho \rightarrow \infty$, $P(S) \xrightarrow{p} Q(S)$.
2. Fix ρ and let $S = S_1 \times S_2$, where $S_v \in \mathcal{S}_v$ and $H_v(S_v) > 0$ for $v = 1, 2$. Then as $\gamma_1, \gamma_2 \rightarrow \infty$, $P(S) \xrightarrow{d} P_0(S)$ where $P_0 \sim \text{DP}(\rho, H_1 \times H_2)$.

Proposition 1 states that in limiting cases for the concentration parameters, the PCDP converges to either a DP with a product base measure or the product measure of two independent DP measures. The first statement follows after applying Markov's inequality to show that for any $\epsilon > 0$ and $\rho > 0$, $\pi(|P(S) - Q(S)| > \epsilon \mid \rho) \leq 1/\{4\epsilon^2(\rho + 1)\}$. We verify the second statement by proving convergence of the CDF for $P(S)$ conditional on $Q_1(S_1)$ and $Q_2(S_2)$, then applying the dominated convergence theorem. Therefore, the choices of ρ , γ_1 , and γ_2 are very important for the distribution of the random partitions. We will return to the effect of the concentration parameters on inference in Section 3, where we show that in the PCDP, the dependence between C_1 and C_2 is modeled as a function of these values.

The PCDP can be extended to $V \geq 2$ views by setting $Q = \times_{v=1}^V Q_v$, where $Q_v \mid \gamma_v, H_v \sim \text{DP}(\gamma_v, H_v)$, then sampling $P \mid \rho, Q$ from (7). Here, ρ can be interpreted as a global clustering dependence parameter, i.e., the dependence structure between each pair (C_v, C_u) is identical for all $v \neq u$. Additionally, a similar Pólya urn scheme to (11) holds in the general case, where past combinations are weighted by entries in the contingency array $\mathbf{n} = (n_{k_1 \dots k_V})_{k_1, \dots, k_V}$ and the customer now has V choices to make when they enter the restaurant. Accordingly, the V -view cross-partition is defined as $D = (D_{k_1 \dots k_V})_{v=1, \dots, V}$, where $D_{k_1 \dots k_V} = \bigcap_{v=1}^V C_{vk_v}$. We can recover the contingency tables for any two views by summing along the dimensions of \mathbf{n} , and we can construct the associated 2-view cross-partitions by taking unions of the sets in D . By Fubini's theorem, the univariate marginals of P follow an HDP, and pairwise marginals are distributed as PCDPs with two views. Therefore, results from the two view case will carry over to any pairs of views in the V -partition setting.

2.3 FINITE APPROXIMATION

Draws from the PCDP are random measures with a countably infinite number of support points, i.e. $P = \sum_{k_1=1}^{\infty} \sum_{k_2=1}^{\infty} p_{k_1 k_2} \delta_{(\theta_{1k_1}^*, \theta_{2k_2}^*)}$. However, this makes simulation and inference on P computationally infeasible. In this section, we propose a finite measure $\tilde{P} = \sum_{k_1=1}^{L_1} \sum_{k_2=1}^{L_2} \tilde{p}_{k_1 k_2} \delta_{(\tilde{\theta}_{1k_1}^*, \tilde{\theta}_{2k_2}^*)}$, where $L_1, L_2 < \infty$, which approximates P as L_1 and L_2 grow large. Our method is similar to the approximation to the DP prior given by sampling a L -dimensional $p \sim \text{Dir}(\rho/L, \dots, \rho/L)$ and $\theta_l^* \sim Q$ for $l = 1, \dots, L$, then taking $L \rightarrow \infty$ (Ishwaran and Zarepour, 2002; Lijoi et al., 2023). Teh et al. (2006) showed several finite approximations to the HDP using the Dirichlet-multinomial distribution, which we adapt for the PCDP. The finite PCDP is given by

$$\begin{aligned} \tilde{p} \mid \rho, \tilde{q} &\sim \text{Dir}(\rho \tilde{q}); & \tilde{q} &= \tilde{q}_1 \otimes \tilde{q}_2; \\ \tilde{q}_v &\sim \text{Dir}(\gamma_v/L_v, \dots, \gamma_v/L_v), & \tilde{\theta}_{vk_v}^* &\sim H_v \text{ for } v = 1, 2; \end{aligned} \tag{12}$$

where \otimes denotes the tensor product, i.e. $\tilde{q} = (\tilde{q}_{1k_1} \tilde{q}_{2k_2})_{k_1, k_2}$, and $k_v = 1, \dots, L_v$. We denote $\tilde{Q}_v = \sum_{k_v=1}^{L_v} \tilde{q}_{vk_v} \delta_{\tilde{\theta}_{vk_v}^*}$ to be the approximation of \tilde{Q}_v and set $\tilde{Q} = \tilde{Q}_1 \times \tilde{Q}_2$. Using Fubini's theorem and results on DP approximations (Ishwaran and Zarepour, 2002), we obtain the following result on convergence of \tilde{Q} to Q . Our result is stated in terms of the expectation of a bounded measurable function $h(\theta)$. We denote $\iint h(\theta) d\tilde{Q}(\theta) = \mathbb{E}_{\tilde{Q}}[h(\theta)]$ and $\iint h(\theta) dQ(\theta) = \mathbb{E}_Q[h(\theta)]$.

Proposition 2. Let $h : \Theta \rightarrow \Theta' \subset \mathbb{R}$ so that $h(\theta) = h_1(\theta_1)h_2(\theta_2)$, $h_v(\cdot)$ is $(\Theta_v, \mathcal{S}_v)$ -measurable for $v = 1, 2$, and h is bounded on Θ . Then, as $L_1, L_2 \rightarrow \infty$,

$$\int \int h(\theta) d\tilde{Q}(\theta) \xrightarrow{d} \int \int h(\theta) dQ(\theta). \quad (13)$$

With regard to \tilde{P} , observe that, as in the infinite case, $\tilde{P} \mid \rho, \tilde{Q} \sim \text{DP}(\rho, \tilde{Q})$: if S_1, \dots, S_K is a partition of Θ , then $(\tilde{P}(S_1), \dots, \tilde{P}(S_M)) \mid \rho, \tilde{Q} \sim \text{Dir}(\rho\tilde{Q}(S_1), \dots, \rho\tilde{Q}(S_M))$, where $\tilde{Q}(S_m) = \sum_{k_1, k_2} \mathbf{1}_{(\tilde{\theta}_{1k_1}^*, \tilde{\theta}_{2k_2}^*) \in S_m} \tilde{q}_{1k_1} \tilde{q}_{2k_2}$. Examples of functions h satisfying the conditions of Proposition 2 are the CDFs of X_i in the correlated and uncorrelated views models, i.e. (5) and (6). This shows that the distribution of X_i under the finite model will resemble the infinite case as $L_1, L_2 \rightarrow \infty$. For example, the expected CDF of X_i in the finite approximation is $\tilde{\mathbb{E}}[\tilde{\Pi}(x_i \mid \tilde{P}) \mid \tilde{Q}] = \int \int F(x_i; \theta) d\tilde{Q}(\theta)$ and in the regular PCDP is $\mathbb{E}[\Pi(x_i \mid P) \mid Q] = \int \int F(x_i; \theta) dQ(\theta)$, where $F(x_i; \theta)$ is the CDF for $f(x_i; \theta)$. Then, (13) implies that $\tilde{\mathbb{E}}[\tilde{\Pi}(x_i \mid \tilde{P}) \mid \tilde{Q}] \xrightarrow{d} \mathbb{E}[\Pi(x_i \mid P) \mid Q]$.

Properties from the infinite PCDP carry over into the finite approximation. For example, the marginals \tilde{P}_v of \tilde{P} are distributed as finite approximations to the HDP, and using a similar argument to the one above, we can show that these provide accurate approximations to the view-specific marginal CDFs. In Section 4, we derive a Gibbs sampler for multiview and conditional models using the finite approximation in (12). In practice, we recommend setting L_1 and L_2 to be large positive integers that serve as prior beliefs on an upper bound to the number of clusters K_1 and K_2 along the views. We will show in the following section that the expectation of the Rand index for the finite approximation converges to that of the PCDP at a $(L_1 L_2)^{-1}$ rate.

3 CLUSTERING WITH INDEPENDENCE CENTRING

Recall that ties in θ_{vi} generate a partition $C_v = (C_{v1}, \dots, C_{vK_v}) \in \mathcal{P}_n$ for $v = 1, 2$. In this section, we address the induced joint distribution of (C_1, C_2) , which we denote as $\text{CLIC}(\rho, \gamma_1, \gamma_2)$. We will show that the joint distribution of (C_1, C_2) depends only on the contingency table $\mathbf{n} = (n_{k_1 k_2})_{k_1, k_2}$, where $n_{k_1 k_2} = |C_{1k_1} \cap C_{2k_2}|$. This behavior is comparable to an exchangeable partition probability function (EPPF), a special type of PMF for random partitions that is an exchangeable function of the cluster sizes (Pitman, 2002). The cluster sizes can be recovered via summation, i.e. $n_{1k_1} = \sum_{k_2} n_{k_1 k_2}$ (row summation) and $n_{2k_2} = \sum_{k_1} n_{k_1 k_2}$ (column summation). The CRP(γ) distribution in (2) is an example of an EPPF, though partitions induced by Pitman-Yor processes, symmetric

Dirichlet-Multinomial sampling, and even hierarchical processes such as the HDP also admit EPPFs (Camerlenghi et al., 2018, 2019). The telescopic EPPF (Franzolini et al., 2023) is a generalization of EPPFs to multiview clustering, and closed-form expression of telescopic EPPFs exist for several multiview clustering models.

We say that the joint partition function of (C_1, C_2) is a marginally exchangeable partition probability function (MEPPF) if $\pi(C_1, C_2)$ is a function of the contingency table \mathbf{n} that is invariant to permutations of the *marginal* cluster indices. For example, permutations of the rows or columns of the contingency table will result in the same prior probability, i.e. if $\pi(C_1, C_2) = g(\mathbf{n})$ and if ω is a permutation of $[K_1]$ and $\mathbf{n}^\omega = (n_{\omega(k_1), k_2})_{k_1, k_2}$, then $g(\mathbf{n}) = g(\mathbf{n}^\omega)$; an identical guarantee holds for permutations of $[K_2]$. Observe that exchangeability of the marginal cluster indices is not equivalent to exchangeability of the entries in \mathbf{n} . Pragmatically, this is to ensure that we can always recover the marginal cluster sizes by summing along the rows or columns of \mathbf{n} . We now present the closed-form expression for the MEPPF of the CLIC(ρ, γ_1, γ_2) distribution.

Theorem 2. Suppose \mathcal{S}_v is the Borel algebra of Θ_v for $v = 1, 2$. If $(C_1, C_2) \sim \text{CLIC}(\rho, \gamma_1, \gamma_2)$, then

$$\pi(C_1, C_2 \mid \rho, \gamma_1, \gamma_2) = \frac{\gamma_1^{K_1} \gamma_2^{K_2}}{(\rho)^{(n)}} \sum_{\mathbf{r} \in \mathcal{R}} \rho^r \left\{ \prod_{v=1}^2 \frac{\prod_{k_v} (r_{vk_v} - 1)!}{(\gamma_v)^{(r)}} \right\} \prod_{k_1, k_2} |s(n_{k_1 k_2}, r_{k_1 k_2})|, \quad (14)$$

where $(\rho)^{(n)} = \Gamma(\rho + n)/\Gamma(\rho)$, $\mathcal{R} = \{\mathbf{r} = (r_{k_1 k_2})_{k_1, k_2} : r_{k_1 k_2} \in [n_{k_1, k_2}] \forall k_1, k_2\}$, $r = \sum_{k_1, k_2} r_{k_1 k_2}$, $r_{1k_1} = \sum_{k_2} r_{k_1 k_2}$, $r_{2k_2} = \sum_{k_1} r_{k_1 k_2}$, and $|s(n, m)|$ are the unsigned Stirling numbers of the first kind.

We present the proof of Theorem 2 in the Supplemental Material; the result follows by adapting the derivations of Camerlenghi et al. (2018) on the EPPF induced by the HDP and exploiting the product measure formulation of Q and the prior independence of Q_1 and Q_2 . Observe that $\pi(C_1, C_2 \mid \rho, \gamma_1, \gamma_2)$ is itself a mixture model over independent contingency tables in \mathcal{R} , given by the *root partitions* T_1 and T_2 . First, we sample $r \in [n]$ via $\pi(r = w \mid \rho) \propto \rho^w$ for $w = 1, \dots, n$, then we sample two partitions of $[r]$ from

$$\pi(T_1, T_2 \mid \gamma_1, \gamma_2) = \prod_{v=1}^2 \frac{\gamma_v^{K_v} \prod_{k_v} (r_{vk_v} - 1)!}{(\gamma_v)^{(r)}}, \quad (15)$$

which is the product of the EPPFs for two independent CRP(γ_v) partitions. Finally, we sample (C_1, C_2) conditionally on (T_1, T_2) from

$$\pi(C_1, C_2 \mid \rho, \gamma_1, \gamma_2, T_1, T_2) \propto \frac{\Gamma(\rho)}{\Gamma(n + \rho)} \prod_{k_1, k_2} |s(n_{k_1 k_2}, r_{k_1 k_2})|. \quad (16)$$

Hence, we can reinterpret the data generating process as first drawing two root partitions, then perturbing their cross partition using the probability mass function in (16). An important consequence of this decomposition is that

$$\pi(K_v = m \mid \rho, \gamma_v) = \begin{cases} \sum_{w=1}^n \frac{\rho^{w-1}(1-\rho)}{1-\rho^n} \Pr[K(w; \gamma_v) = m] & \text{for } \rho \neq 1; \\ \frac{1}{n} \sum_{w=1}^n \Pr[K(w; \gamma_v) = m] & \text{for } \rho = 1; \end{cases}, \quad (17)$$

where $K(w; \gamma_v)$ is the number of clusters in a sample of w objects from a CRP(γ_v) distribution, see [Antoniak \(1974\)](#) and [Gnedin and Pitman \(2006\)](#) for further information on this quantity. Therefore, both ρ and γ_v impact the number of clusters in the marginals. As $\rho \rightarrow \infty$, $\rho^{n-1}(1-\rho)/(1-\rho^n) \rightarrow 1$, meaning that $K_v \xrightarrow{d} K(n; \gamma_v)$, as expected by our discussion in the previous section. Finally, K_v grows very slowly with the sample size a priori, as it has been shown that the number of clusters in an HDP scales asymptotically at a $\log \log n$ rate ([Teh and Jordan, 2010](#); [Camerlenghi et al., 2019](#)).

The marginal distributions of P in (10) imply that C_1 and C_2 are both distributed as HDP partitions, and if $\gamma_1 = \gamma_2$, then $C_1 \stackrel{d}{=} C_2$. The EPPF of C_v is then given by

$$\pi(C_v \mid \rho, \gamma_v) = \frac{\gamma_v^{K_v}}{(\rho)^{\binom{n}{K_v}}} \sum_{\mathbf{r}_v \in \mathcal{R}_v} \frac{\rho^r}{(\gamma_v)^{\binom{r}{K_v}}} \prod_{k_v=1}^{K_v} (r_{vk_v} - 1)! |s(n_{vk_v}, r_{vk_v})|, \text{ for } v = 1, 2; \quad (18)$$

where the domain of the sum is $\mathcal{R}_v = \{\mathbf{r}_v = (r_{v1}, \dots, r_{vK_v}) : r_{vk_v} \in [n_{vk_v}], k_v = 1, \dots, K_v\}$ ([Camerlenghi et al., 2018](#)). Similar to the joint distribution, the marginals admit a conditional sampling scheme given a root partition T_v . As we also showed in (17), ρ affects not only the joint distribution of the partitions but also the marginals. This phenomenon is evident in the Pólya urn scheme in (11). The probability of choosing a table and dish independently, which includes the possibility of picking a new table or dish, is controlled by ρ . Hence, for very small ρ , the number of clusters in both C_1 and C_2 is expected to be small.

Following [Page et al. \(2022\)](#) and [Franzolini et al. \(2023\)](#), we use the prior expected Rand index (ERI) $\tau_{12} = \sum_{C_1, C_2 \in \mathcal{P}_n} R(C_1, C_2) \pi(C_1, C_2 \mid \rho, \gamma_1, \gamma_2)$ to measure dependence between C_1 and C_2 . For convenience, we will assume that $\gamma_1 = \gamma_2 = \gamma$, but a similar result holds for differing values of γ_v . For two independent CRP partitions, their ERI is given by $\tau_{12}^0 = (1 + \gamma^2)/(1 + \gamma)^2$ ([Page et al., 2022](#)). Under the PCDP, the ERI is a weighted average between the ERI of two independent CRP partitions and 1, the supremum of the Rand index.

Theorem 3. Let $(C_1, C_2) \sim \text{CLIC}(\rho, \gamma, \gamma)$. Then,

$$\tau_{12} = \frac{1}{\rho + 1} + \left(1 - \frac{1}{\rho + 1}\right) \frac{1 + \gamma^2}{(1 + \gamma)^2}. \quad (19)$$

Our intuition on the magnitude of the concentration parameters carries over to the ERI. As $\rho \rightarrow \infty, \tau_{12} \rightarrow (1 + \gamma^2)/(1 + \gamma)^2$, whereas if $\gamma \rightarrow \infty, \tau_{12} \rightarrow 1$. While the Rand index is guaranteed to be in $[0, 1]$, we have that $(1 + \gamma^2)/(1 + \gamma)^2 \leq \tau_{12} \leq 1$. Similar truncation occurs in several models for clustering, which motivated the adjusted Rand index (ARI) (Hubert and Arabie, 1985) and, more recently, the telescopic adjusted Rand index (TARI) (Franzolini et al., 2023), which removes the lower bound imposed by the independent model. In the latter case, we have that the expected TARI is simply equal to $\nu = 1/(\rho + 1)$ under the PCDP.

Recall that γ controls the choices of customer i in selecting a table and entrée, with large γ leading to trivial dependence between C_1 and C_2 . We now have the added interpretation that γ determines the ERI of the null independence model. That is, the ERI between C_1 and C_2 will be at least as large as the ERI between two independent $\text{CRP}(\gamma)$ partitions. If we assign ρ and γ priors, we induce a prior directly on τ_{12} . Since γ is the DP concentration parameter of Q_1, Q_2 and ρ is the DP concentration parameter of $P | Q$, we can model both using semi-conjugate prior distributions, such as a Gamma prior (Escobar and West, 1995) or a Stirling-Gamma prior (Zito et al., 2023). Then, samples from the posterior distribution for the ERI $\pi(\tau_{12} | \mathbf{X})$ can be obtained from the samples of ρ, γ .

A similar result on the ERI holds for the finite approximation to CLIC. In this setting, we sample C_1, C_2 using a matrix multinomial distribution, with $\tilde{\pi}(c_{1i} = k_1, c_{2i} = k_2 | \tilde{p}) = \tilde{p}_{k_1 k_2}$ for all $k_1 = 1, \dots, L_1, k_2 = 1, \dots, L_2$. We show in the Supplement that if $\tilde{\tau}_{12}$ is the ERI resulting from the model in (12), then $\tilde{\tau}_{12} = \nu + (1 - \nu)\kappa(L_1, L_2)$, where $\kappa(L_1, L_2)$ is the ERI of two independent partitions with symmetric Dirichlet-multinomial priors and $\lim_{L_1, L_2 \rightarrow \infty} \kappa(L_1, L_2) = (1 + \gamma^2)/(1 + \gamma)^2$. This result also provides insight on the impact of setting L_1 and L_2 to finite values. For simplicity, suppose that $L_1 = L_2 = L$ for some fixed $L > 0$. One can show that $|\tau_{12} - \tilde{\tau}_{12}| \propto |(\gamma/L) + 1 - \gamma|/L$, where proportionality is in terms of L . That is, the rate of convergence for the ERI of the finite approximation to the PCDP is quadratic in L^{-1} .

4 POSTERIOR COMPUTATION

4.1 GIBBS SAMPLER

Given a dataset \mathbf{X} and a multiview clustering model such as (5) or (6), we focus on inferring the view-specific partitions (C_1, C_2) and estimating the degree of dependence between the partitions using the Rand index or the TARI. Since the PCDP as presented in Section 2 has infinitely many mixture components, we present an algorithm specific to the finite approximation in (12). We will assume that H_v are conjugate to the kernels in either (5) or (6), and that $\rho \sim \text{Gamma}(a_\rho, b_\rho)$ for some $a_\rho, b_\rho > 0$ or $\pi(\rho = u) \propto 1$ for a set of finite numbers u defined on a grid U , leading to a griddy-Gibbs sampler (Ritter and Tanner, 1992). The key strategy in our approach is to marginalize out the probability matrix \tilde{p} from the multinomial likelihood of (C_1, C_2) , similar to posterior inference on the finite approximation to the HDP (Teh et al., 2006). This leads to a Gibbs sampler for the two view setting, but computation is similar when there are $V > 2$ views.

Let K_v be the number of non-empty clusters in C_v , where $K_v \leq L_v$ for $v = 1, 2$. By marginalizing \tilde{p} from $\pi(C_1, C_2 | \tilde{p}, \rho)$, one can show that the prior probability mass function of (C_1, C_2) is given by

$$\pi(C_1, C_2 | \tilde{q}, \rho) = \frac{\Gamma(\rho)}{\Gamma(n + \rho)} \prod_{k_1=1}^{L_1} \prod_{k_2=1}^{L_2} \frac{\Gamma(n_{k_1 k_2} + \rho \tilde{q}_{1k_1} \tilde{q}_{2k_2})}{\Gamma(\rho \tilde{q}_{1k_1} \tilde{q}_{2k_2})}, \quad (20)$$

where $n_{k_1 k_2} = 0$ if either $k_1 > K_1$ or $k_2 > K_2$. Denote C_1^{-i} and C_2^{-i} to be the partitions induced on $[n] \setminus \{i\}$ by removing observation i . We have that $\pi(c_{1i} = k_1, c_{2i} = k_2 | C_1^{-i}, C_2^{-i}, \tilde{q}, \rho) \propto \rho \tilde{q}_{1k_1} \tilde{q}_{2k_2} + n_{k_1 k_2}^{-i}$, where $n_{k_1 k_2}^{-i} = \sum_{j \neq i} \mathbf{1}(c_{1j} = k_1, c_{2j} = k_2)$ for all $k_1 \in [K_1], k_2 \in [K_2]$ and $n_{k_1 k_2}^{-i} = 0$ if either $k_1 > K_1$ or $k_2 > K_2$. The Gibbs update of observation i is given by the formula

$$\pi(c_{1i} = k_1, c_{2i} = k_2 | -) \propto f(X_i; (\theta_{1k_1}^*, \theta_{2k_2}^*)) (\rho \tilde{q}_{1k_1} \tilde{q}_{2k_2} + n_{k_1 k_2}^{-i}), \quad (21)$$

for all $k_1 \in [L_1], k_2 \in [L_2]$, where “-” refers to $C_1^{-i}, C_2^{-i}, \tilde{q}, \rho, \theta_{1k_1}^*, \theta_{2k_2}^*$, and \mathbf{X} .

In order to sample the full conditional distribution of \tilde{q}_1, \tilde{q}_2 , and ρ , we adapt an auxiliary variable scheme used for inference on HDPs to our model (Teh et al., 2006). By using properties of the Gamma function, one can show that the product terms in (20) can be decomposed in the following way for all

$k_1 \in [K_1], k_2 \in [K_2]$,

$$\frac{\Gamma(n_{k_1 k_2} + \rho \tilde{q}_{1k_1} \tilde{q}_{2k_2})}{\Gamma(\rho \tilde{q}_{1k_1} \tilde{q}_{2k_2})} = \sum_{r_{k_1 k_2}=0}^{n_{k_1 k_2}} |s(n_{k_1 k_2}, r_{k_1 k_2})| (\rho \tilde{q}_{1k_1} \tilde{q}_{2k_2})^{r_{k_1 k_2}},$$

where $|s(n, m)|$ are the unsigned Stirling numbers of the first kind. We can rewrite (20) as being the marginals of the following joint distribution based on a matrix $\mathbf{r} = (r_{k_1 k_2})_{k_1, k_2}$ of auxiliary variables,

$$\Pi(C_1, C_2, \mathbf{r} \mid \tilde{q}_1, \tilde{q}_2, \rho) = \frac{\Gamma(\rho)}{\Gamma(n + \rho)} \prod_{k_1=1}^{K_1} \prod_{k_2=1}^{K_2} |s(n_{k_1 k_2}, r_{k_1 k_2})| (\rho \tilde{q}_{1k_1} \tilde{q}_{2k_2})^{r_{k_1 k_2}}. \quad (22)$$

Note that these auxiliary variables correspond to the domain of summation in the MEPPF (14) for the PCDP, and that the product is over all non-empty clusters. Similarly, we define clustering-specific auxiliary variables $r_{1k_1} = \sum_{k_2=1}^{K_2} r_{k_1 k_2}$ and $r_{2k_2} = \sum_{k_1=1}^{K_1} r_{k_1 k_2}$. To update $r_{k_1 k_2}$, we sample from a multinomial distribution using

$$\pi(r_{k_1 k_2} = w \mid C_1, C_2, \mathbf{r}^{-k_1 k_2}) \propto |s(n_{k_1 k_2}, w)| (\rho \tilde{q}_{1k_1} \tilde{q}_{2k_2})^w; \quad w \in \{0, 1, \dots, n_{k_1 k_2}\}. \quad (23)$$

We use the recursive formula $|s(n+1, w)| = n|s(n, w)| + |s(n, w-1)|$ to compute the unsigned Stirling numbers of the first kind.

Using (22), we can see that the full conditional distribution of \tilde{q}_v is a $\text{Dir}(\gamma_v/L_v + r_{v1}, \dots, \gamma_v/L_v + r_{vL_v})$, where $r_{vk_v} = 0$ for all $k_v > K_v$, for $v = 1, 2$. This update in particular provides insight onto the interpretation of the auxiliary variables. Consider the independent clustering model, in which $\pi(c_{1i} = k_1, c_{2i} = k_2 \mid \tilde{q}_1, \tilde{q}_2) = \tilde{q}_{1k_1} \tilde{q}_{2k_2}$. Then the Gibbs update of \tilde{q}_1 and \tilde{q}_2 will be exactly the same as in our model, except with \mathbf{r}_1 and \mathbf{r}_2 being replaced with \mathbf{n}_1 and \mathbf{n}_2 . However, in general $r = \sum_{k_1, k_2} r_{k_1 k_2} < n$. We then interpret \mathbf{r} as being the cell counts of C_1 and C_2 if they were modeled as being truly independent and defined on a smaller sample.

If $\rho \sim \text{Gamma}(a_\rho, b_\rho)$, we use a data augmentation technique introduced in Escobar and West (1995). From (20), one sees that the full conditional distribution of ρ is

$$\Pi(\rho \mid C_1, C_2, \mathbf{r}, \tilde{q}_1, \tilde{q}_2, \mathbf{X}) \propto \pi(\rho) \frac{\Gamma(\rho)}{\Gamma(n + \rho)} \rho^r \propto \pi(\rho) \rho^{r-1} (\rho + n) \beta(\rho + 1, n) \quad (24)$$

where $\beta(\cdot, \cdot)$ is the beta function. Since $\beta(\rho + 1, n) = \int_0^1 \eta^\rho (1 - \eta)^{n-1} d\eta$, we have that (24) is the marginal distribution of ρ for a joint density proportional to $\pi(\rho) \rho^{r-1} (\rho + n) \eta^\rho (1 - \eta)^{n-1}$ for $0 < \eta < 1$

and $\rho > 0$. We set η to be an auxiliary variable, then acquire samples from (24) by alternating sampling of η and ρ . We update η by sampling from a $\text{Beta}(\rho + 1, n)$ distribution. To sample ρ , we simulate from a two-component mixture of Gamma distributions: $\omega_\eta \text{Gamma}(a_\rho + r, b_\rho - \log \eta) + (1 - \omega_\eta) \text{Gamma}(a_\rho + r - 1, b_\rho - \log \eta)$, where $\omega_\eta / (1 - \omega_\eta) = (a_\rho + r - 1) / \{n(b_\rho - \log \eta)\}$. If instead $\pi(\rho = u) \propto 1$ for all $u \in U$, we update the position of ρ by simulating from a discrete distribution proportional to (20) for all points on the grid.

Finally, to update $\theta_{vk_v}^*$, we sample from $\pi(\theta_{vk_v} | \mathbf{C}_v, \mathbf{X}) \propto \left\{ \prod_{i \in C_{vk_v}} \pi(X_i; \theta_{vk_v}^*) \right\} H_v(\theta_{vk_v}^*)$ for $k_v = 1, \dots, K_v$, where in independent view case, $\pi(X_i; \theta_{vk_v}^*) = f_v(X_{vi}; \theta_{vk_v}^*)$, and in the correlated case, $\pi(X_i; \theta_{1k_1}^*) = f_1(X_{1i}; \theta_{1k_1}^*)$ and $\pi(X_i; \theta_{2k_2}^*) = f_2(X_{2i}; X_{1i}, \theta_{2k_2}^*)$. For any $k_v > K_v$, where $n_{vk_v} = 0$, we simulate $\theta_{vk_v}^* \sim H_v$.

4.2 POINT ESTIMATION AND UNCERTAINTY QUANTIFICATION

At the termination of the Gibbs sampler we obtain MCMC samples $C_1^{(t)}, C_2^{(t)} \sim \pi(C_1, C_2 | \mathbf{X})$ for $t = 1, \dots, T$ iterations. We compute point estimates $\{\hat{C}_v\}$ of the partitions by minimizing the posterior expectation of a clustering loss function. In our simulations and application, we use the Variation of Information (VI) loss (Meilă, 2007), though alternatives exist including Binder’s loss (Binder, 1978) and generalized losses (Dahl et al., 2022). As in the single view case, we would expect kernel misspecification in the PCDP to result in over-clustering the data by approximating true clusters with several mixture components. One strategy to robustify inference on the partitions is to apply a kernel merging algorithm to the marginals such as Fusing of Localized Densities (FOLD) (Dombowsky and Dunson, 2023), which takes the posterior samples of θ_{1i} and θ_{2i} as input. One could also implement the PCDP as a prior to infer the coarsened posterior of the partitions, an inferential framework which allows for perturbations in the observed data from the assumed component kernels (Miller and Dunson, 2019).

Uncertainty in clustering is conveyed with either the posterior similarity matrix, which measures $\pi(c_{vi} = c_{vj} | \mathbf{X})$ for all i, j pairs, or a credible ball (Wade and Ghahramani, 2018), which provides a set of clusterings close to \hat{C}_v in the partition metric space that have high posterior probability. To quantify dependence in the partitions, we infer $\pi\{R(C_1, C_2) | \mathbf{X}\}$ or, alternately, the posterior of the TARI, and provide the posterior mean and a credible interval. For inference on the number of clusters in the v th view, we calculate the posterior probability of any $\hat{K}_v > 0$ with $\pi(K_v = \hat{K}_v |$

\mathbf{X}) $\approx (1/T) \sum_{t=1}^T \mathbf{1}_{K_v^{(t)}=\hat{K}_v}$, where $K_v^{(t)} = \sum_{k_v=1}^{L_v} \mathbf{1}_{C_{vk_v}^{(t)} \neq \emptyset}$ counts the number of non-empty blocks in the v th partition. For interpretability, we recommend inspecting the marginal posterior distributions of K_1 and K_2 individually, though inferences on their joint distribution can also be obtained with $\pi(K_1 = \hat{K}_1, K_2 = \hat{K}_2 | \mathbf{X}) \approx (1/T) \sum_{t=1}^T \mathbf{1}_{K_1^{(t)}=\hat{K}_1, K_2^{(t)}=\hat{K}_2}$.

5 ILLUSTRATIONS

5.1 TWO VIEW SETTING

To evaluate the performance of CLIC and the PCDP relative to competitors, we simulate $n = 200$ observations under three cases of partition dependence between two views: identical clusterings (case 1), dependent clusterings (case 2), and independent clusterings (case 3). In all cases, we set the number of true clusters in each view to be $K_1 = K_2 = 2$, and simulate C_1 via $\Pr(c_{1i} = 1) = \Pr(c_{1i} = 2) = 1/2$. In case 1, we set $c_{2i} = c_{1i}$, and in case 3 we simulate c_{2i} independently using $\Pr(c_{2i} = 1) = \Pr(c_{2i} = 2) = 1/2$. For case 2, with probability $2/3$ we sample (c_{1i}, c_{2i}) using the scheme in case 1, and with probability $1/3$ we sample (c_{1i}, c_{2i}) independently with the scheme in case 3. We focus on the uncorrelated view model (5), but we also explore the correlated view model (6) in the Supplementary Material.

When fitting the PCDP, we fix $\gamma_1 = \gamma_2 = 1$, but assume that $\rho \sim \text{Gamma}(1, 1)$. We run the Gibbs sampler in Section 4 for 30,000 iterations, remove the first 10,000 as burn-in, then keep every other iteration, leading to 10,000 samples from $\pi(C_1, C_2 | \mathbf{X})$. We find that mixing improves using a conditional sampling scheme for the cluster labels. Rather than sampling (c_{1i}, c_{2i}) jointly from its full conditional, we first sample c_{1i} , then c_{2i} conditional on the value of c_{1i} . We also find that this method vastly speeds up posterior computation in comparison to the joint sampler. Mixing and convergence of the PCDP are evaluated using traceplots and effective sample size for $R(C_1, C_2)$.

CLIC is compared to existing methods for clustering uncorrelated views. We evaluate the model in (5) across two different overlaps in the sample space for the C_2 clusters. That is, we generate data via $(X_i | c_{1i}, c_{2i}) \sim \mathcal{N}(X_{1i}; \{-1\}^{c_{1i}+1}, 0.2) \times \mathcal{N}(X_{2i}; \{-1\}^{c_{2i}}, \eta^2)$, where $\eta^2 \in \{0.2, 0.45\}$. Smaller values of η^2 lead to wider separation along the second view. Plots of the synthetic data are displayed in Figure 1. We fit a location Gaussian mixture with the finite approximation to the PCDP, i.e. $\pi(X_i | \theta_i) = \mathcal{N}(X_{1i}; \theta_{1i}, \sigma_1^2) \times \mathcal{N}(X_{2i}; \theta_{2i}, \sigma_2^2)$, and assume that $H_v(\theta) = \mathcal{N}(\theta; \mu_0, \sigma_0^2)$. We then compute the clustering point estimates corresponding to the telescopic hierarchical Dirichlet process

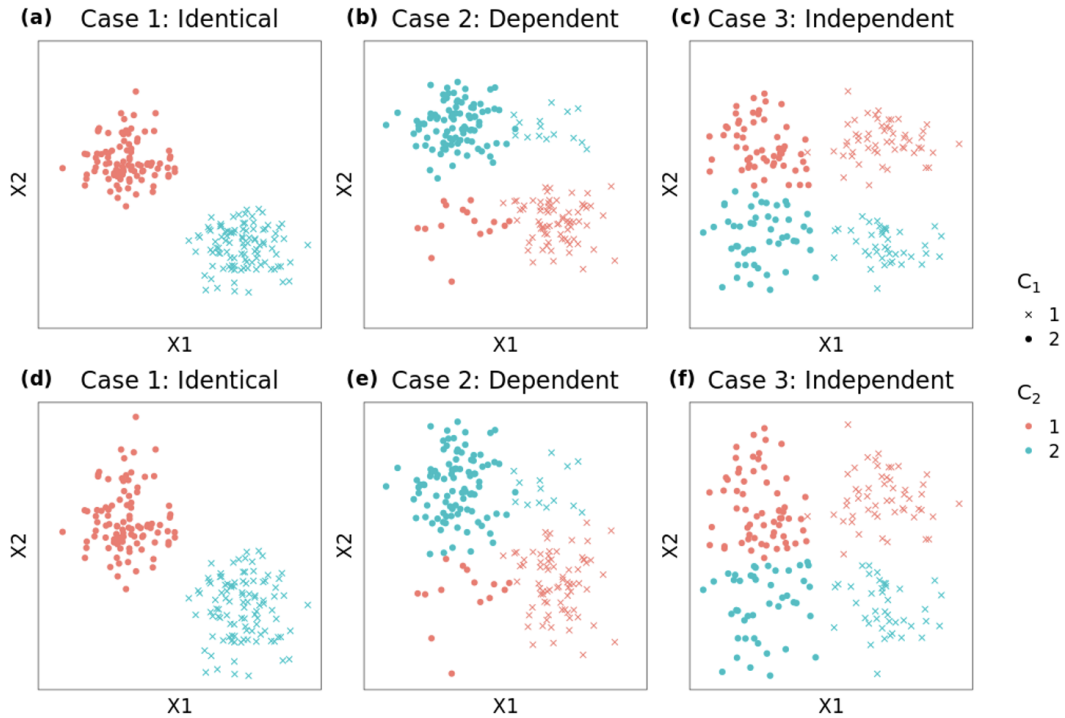


Figure 1: Synthetic data simulated in the two view setting, where shapes and colors correspond to the true values of C_1 and C_2 . Data in plots (a)-(c) are simulated with little overlap between C_2 clusters ($\eta^2 = 0.2$), whereas data in plots (d)-(f) are simulated with higher overlap ($\eta^2 = 0.45$).

(t-HDP) described in [Franzolini et al. \(2023\)](#), two independent Dirichlet processes (IDPs), and the EM algorithm ([Scrucca et al., 2023](#)) applied independently to each view. In all Bayesian methods, point estimates are calculated with the VI loss.

The ARI between the point estimates and the true partitions are displayed in [Table 1](#). All methods perform similarly when the clusters along both views are well separated ($\eta^2 = 0.2$). However, CLIC far more accurately captures C_2 in comparison to competitors after increasing the overlap ($\eta^2 = 0.45$). In case 1, IDPs and the EM algorithm along the marginals completely fail to detect any clustering structure in C_2 . The t-HDP has similar issues in case 3, as its point estimate allocates all objects to a single cluster. Though all methods detect clustering structure in case 2, CLIC attains the highest ARI with the true C_2 clusters, particularly in comparison to the t-HDP. Additionally, CLIC’s estimation of C_1 is consistent across the two different overlaps, but estimation of C_1 in case 2 under the t-HDP worsens when the overlap between the C_2 clusters is increased. We also calculated the number of clusters along each view for each method. When $\eta^2 = 0.2$, all methods estimate the correct number of clusters along both views for all three cases. For $\eta^2 = 0.45$, the EM algorithm and IDPs infer one cluster in the second view in case 1. Similarly, the t-HDP results in one cluster along view 2 in case

Overlap	Case	CLIC	t-HDP	EM	IDPs
$\eta^2 = 0.2$	1	(1.000, 1.000)	(1.000, 1.000)	(1.000, 0.980)	(1.000, 0.980)
	2	(0.921, 0.98)	(0.902, 0.98)	(0.921, 1.000)	(0.921, 1.000)
	3	(0.980, 0.921)	(0.980, 0.921)	(0.980, 0.941)	(0.980, 0.941)
$\eta^2 = 0.45$	1	(1.000, 1.000)	(1.000, 1.000)	(1.000, 0.000)	(1.000, 0.000)
	2	(0.921, 0.921)	(0.883, 0.773)	(0.921, 0.864)	(0.921, 0.864)
	3	(0.980, 0.704)	(0.980, 0.000)	(0.980, 0.687)	(0.980, 0.687)

Table 1: The adjusted Rand indices (ARI) between the true (C_1, C_2) and the point estimates computed by CLIC, the t-HDP, independent EM, and two IDPs for synthetic data in the two view setting. CLIC consistently outperforms competitors for inferring C_2 at a higher overlap.

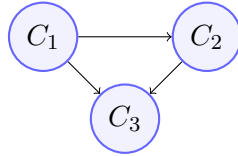


Figure 2: Directed acyclic graph (DAG) formulation for the joint distribution of the simulated partitions (C_1, C_2, C_3) . Note that the DAG is not a tree; C_3 has both C_1 and C_2 as parents.

3. For all other methods and cases under this overlap, the number of clusters along both views are correctly estimated.

5.2 THREE VIEW SETTING

Next, we examine the performance of CLIC and competitors in the three view setting. We set $K_1 = K_2 = K_3 = 2$ to be the number of true clusters and simulate $n = 200$ observations. Here, we only consider the case in which the three partitions are dependent, but not identical. c_{1i} is simulated in the same manner as the two view setting. With probability $1/3$, we set $c_{2i} = c_{1i}$, else we reallocate object i to the other cluster. To simulate c_{3i} , we first generate $u_i \sim \text{Unif}(0, 1)$. If $u_i < 1/3$, then $c_{3i} = c_{1i}$, if $1/3 \leq u_i < 2/3$, then $c_{3i} = c_{2i}$, and if $u_i \geq 2/3$, we simulate c_{3i} independently from the other labels using the same cluster probabilities as c_{1i} . The directed acyclic graph (DAG) in Figure 2 shows the conditional dependencies between all three simulated partitions. Importantly, the dependence structure between C_1 , C_2 , and C_3 does not correspond to a tree graph, which is how the t-HDP model formulates the joint partition distribution. We simulate the data so that the clusters along C_1 and C_2 are more separated than the clusters along the third view. The data are generated by $(X_i | c_{1i}, c_{2i}, c_{3i}) \sim \mathcal{N}(X_{1i}; \{-1\}^{c_{1i}+1}, 0.2) \times \mathcal{N}(X_{2i}; \{-1\}^{c_{2i}}, 0.2) \times \mathcal{N}(X_{3i}; \{-1\}^{c_{3i}+1}, 2, 1)$. A plot of the synthetic data is given in Figure 3. We fit the finite approximation to the PCDP with three views and set $\pi(X_i | \theta_i) = \mathcal{N}(X_{1i}, \theta_{1i}, \sigma_1^2) \times \mathcal{N}(X_{2i}, \theta_{2i}, \sigma_2^2) \times \mathcal{N}(X_{3i}, \theta_{3i}, \sigma_3^2)$, where $H_v(\theta) = \mathcal{N}(\theta; \mu_0, \sigma_0^2)$.

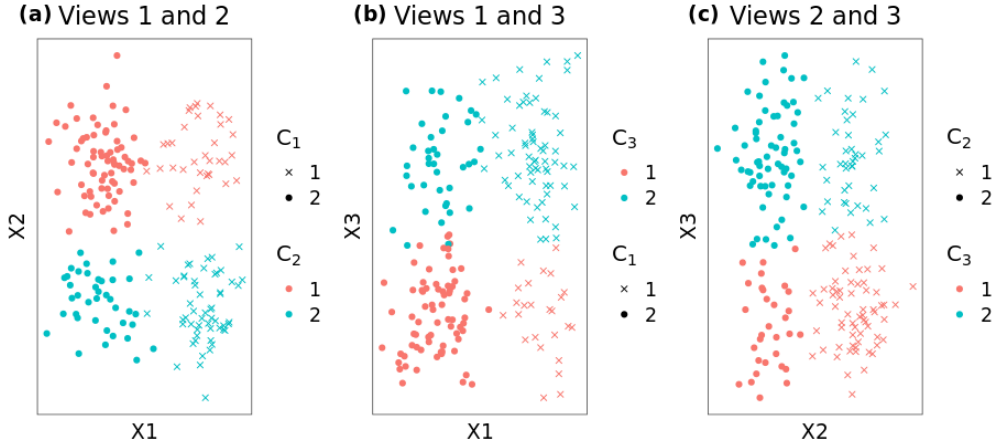


Figure 3: The synthetic data simulated in the three view setting, where shapes and colors correspond to the true values of C_1 , C_2 , and C_3 .

	CLIC	t-HDP	EM	IDPs
ARI with C_1	0.941	0.921	0.941	0.941
ARI with C_2	0.941	0.941	0.941	0.941
ARI with C_3	0.846	0.773	0.827	0.827

Table 2: ARI with the true partitions C_1 , C_2 , and C_3 for point estimates from CLIC, the t-HDP, the EM algorithm, and two IDPs. CLIC attains the joint highest ARI for all partitions, particularly improving on the t-HDP in estimating C_3 .

We draw the same number of posterior samples and keep the same hyperparameters for CLIC, the t-HDP, and the IDPs as in the two view setting. Clustering point estimates are computed with the VI loss function. ARIs between the point estimates from CLIC and the other existing methods are displayed in Table 2. CLIC attains the joint highest ARI with the true partitions, but noticeably improves on the t-HDP in estimating C_3 . This disparity may be explained by the general formulation of dependence in the PCDP: CLIC partitions need not be Markovian or have a tree structure. All methods accurately estimate the number of clusters along the three views.

5.3 VARYING SAMPLE SIZE AND DIMENSION

Finally, we also inspect the performance of our approach and competitors by varying the sample size and dimension of the synthetic data. We simulate two highly dependent partitions, where $c_{2i} = c_{1i}$ with probability $8/10$ (otherwise, the two labels are sampled independently). We fix $d_1 = 2$ but vary $d_2 \in \{2, 10, 25\}$ and $n \in \{100, 200, 500\}$. Along the first view, the true cluster means are $\theta_{11}^* = (1, -1)$, $\theta_{12}^* = (-1, 1)$. Along the second, these are $\theta_{21}^* = (1, -1)_{d_2}$ and $\theta_{22}^* = -\theta_{21}^*$, where $(1, -1)_{d_2}$ is an alternating sequence of ± 1 of length d_2 . We simulate the data via $X_{vi} \mid \theta_{vi} \sim \mathcal{N}(X_{vi}; \theta_{vi}, 0.4I_{d_v})$

$n = 100$					
d_2	CLIC	t-HDP	EM	IDPs	DP
2	(1.000, 0.919) (2,2)	(1.000, 0.919) (2,2)	(1.000, 0.919) (2,2)	(1.000, 0.919) (2,2)	(0.835, 0.783) (4,4)
10	(0.882, 1.000) (2,2)	(0.960, 1.000) (2,2)	(0.845, 1.000) (2,2)	(0.921, 1.000) (2,2)	(0.866, 0.871) (4,4)
25	(0.959,1.000) (2,2)	(1.000,0.143) (2,10)	(0.959,1.000) (2,2)	(0.959,1.000) (2,2)	(0.694,1.000) (2,2)
$n = 200$					
d_2	CLIC	t-HDP	EM	IDPs	DP
2	(0.979,0.939) (2,2)	(0.959,0.939) (2,2)	(0.979,0.899) (2,2)	(0.979,0.899) (2,2)	(0.843,0.826) (4,4)
10	(0.827,1.000) (2,2)	(0.940,1.000) (2,2)	(0.845,1.000) (2,2)	(0.827, 1.000) (2,2)	(0.853, 0.885) (4,4)
25	(0.980,1.000) (2,2)	(1.000,0.927) (2,4)	(0.980,1.000) (2,2)	(0.980,1.000) (2,2)	(0.613,1.000) (2,2)
$n = 500$					
d_2	CLIC	t-HDP	EM	IDPs	DP
2	(0.960,0.960) (2,2)	(0.976,0.944) (2,2)	(0.960,0.944) (2,2)	(0.960,0.944) (2,2)	(0.825,0.806) (4,4)
10	(0.906,1.000) (2,2)	(0.984,1.000) (2,2)	(0.913,1.000) (2,2)	(0.906,1.000) (2,2)	(0.849,0.865) (4,4)
10	(0.968,1.000) (2,2)	(1.000,0.966) (2,4)	(0.968,1.000) (2,2)	(0.960,1.000) (2,2)	(0.822,0.813) (4,4)

Table 3: ARIs (top) and number of clusters (bottom) for CLIC and competitors, where $n \in \{100, 200, 500\}$ and $d_2 \in \{2, 10, 25\}$. For the single view DP, the partition estimates are the same along both views.

independently for $v = 1, 2$. The finite approximation of the PCDP is applied with two independent Gaussian views, $H_v(\theta) = \mathcal{N}_{d_v}(\theta; \mu_0, \Sigma_0)$, $\gamma = 1$, and $\rho \sim \text{Gamma}(1, 1)$. In addition to the competitors used in the previous illustrations, we also fit a single (i.e., ignorant of the views) DP with a Gaussian likelihood to the full data \mathbf{X} .

The resulting ARI values with the true partitions and number of clusters are displayed in Table 3. We can see that CLIC generally performs well at estimating the true cluster labels and always results in the correct number of clusters. Our approach excels in the small sample size but high dimension regime ($n = 100, d_2 = 25$), particularly in the estimation of C_2 . The point estimate of C_2 under CLIC perfectly captures the true partition, whereas the ARI for the t-HDP is 0.143. In general, the t-HDP overestimates the number of clusters along the second view for $d_2 = 25$, resulting in 10 clusters when $n = 100$ and 4 clusters when $n \in \{200, 500\}$. We can also see that CLIC is more robust than a single view DP for estimating both partitions. When $d_2 = 25$ and $n \in \{100, 200\}$, the point estimate for

the DP perfectly corresponds to the C_2 clustering, i.e. the view with dominating dimension, though this tendency is not present in the DP for large n . Finally, it is clear that CLIC can outperform the independent view methods (i.e., EM and IDPs) for smaller values of d_2 .

6 EXAMPLE: THE COLLABORATIVE PERINATAL PROJECT

The Longnecker et al. (2001) dataset is a subset of children studied in the US Collaborative Perinatal Project (CPP) (Niswander and Gordon, 1972). The CPP enrolled pregnant women born between 1959 and 1966, and measured the participants' blood pre-delivery, at delivery, and postpartum. The children of the participants were then monitored for a period of seven years after delivery for neurodevelopmental outcomes. From 1997 to 1999, the Longnecker et al. (2001) study assessed the concentration of DDE, a metabolite of the insecticide DDT, present in blood samples taken from the third trimester using laboratory assays. They were interested in inferring the relationship between DDE concentration and two primary outcomes: preterm delivery and being small-for-gestational age (SGA), the latter term describing newborns with smaller weight than what is considered normal. In total, Longnecker et al. (2001) obtained complete information on 2,380 children, where 361 were classified as being delivered preterm and 221 were small-for-gestational-age.

Following standard procedure in reproductive epidemiology, the two primary outcomes were determined by categorizing birth weight and gestational age. For instance, preterm, term, and post-term births correspond to gestational age at delivery less than 37 weeks, between 37 and 42 weeks, and after 42 weeks, respectively; preterm births are often further classified as very, moderately, or late preterm (Loftin et al., 2010). A baby's birth weight is considered to be low, or "premature", if it does not exceed 2.5 kg (Hughes et al., 2017). There are multiple ways to classify newborns as SGA using birth weight and gestational age, and these generally are study-specific and use percentiles (Schlaudecker et al., 2017). The issue is further complicated by the fact that the start of gestation, and therefore gestational age, is difficult to measure in practice. Therefore, we are interested in inferring *naturally-occurring* subgroups along both birth weight and gestational age, motivating a multiview approach, where view 1 is birth weight and view 2 is gestational age.

The data are collected in the matrix $\mathbf{X} = (\mathbf{X}_1, \mathbf{X}_2)$, where X_{1i} is the normalized birth weight and X_{2i} is the normalized gestational age for child i . We assume that $X_i | \theta_i \sim \mathcal{N}(X_{1i}; \theta_{1i}, \sigma_1^2) \times \mathcal{N}(X_{2i}; \theta_{2i}, \sigma_2^2)$, $\theta_i | P \sim P$, and $P \sim \text{PCDP}$, where the base measures are $H_v(\theta) = \mathcal{N}(\theta; 0, 1)$ and

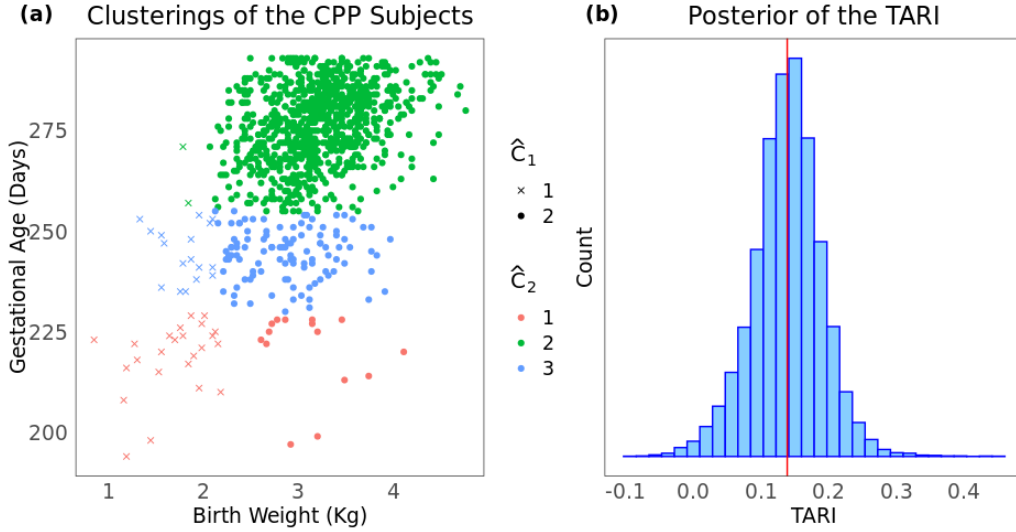


Figure 4: On the left, gestational age and birth weight for the children studied in Longnecker et al. (2001) along with the clustering point estimates, where shapes correspond to groups in birth weight and colors correspond to groups in gestational age. On the right, the posterior distribution of the TARI between C_1 and C_2 , where the red line is the estimated posterior mean (0.139). Note that similar to the ARI, the TARI can take negative values with positive probability.

$\gamma_1 = \gamma_2 = 1$. We take $L_1 = L_2 = 5$ and $\pi(\rho = u) \propto 1$ for all $u \in U$, where U is taken to be a grid from 10^{-2} to 150 in intervals of length 0.5. That is, we implement the griddy-Gibbs sampler discussed in Section 4. We only consider children born before 42 weeks (i.e., full term newborns), then take a random sample of size $n = 1,000$. The Gibbs sampler is run for 100,000 iterations with the first 10,000 taken as burn-in. We take every fifth iteration, leading to 18,000 samples from $\pi(C_1, C_2 | \mathbf{X})$. The griddy-Gibbs sampler leads to better MCMC diagnostics compared to the Escobar and West (1995) semi-conjugate prior for ρ . Convergence of the partitions and ρ was rapid and mixing was good based on trace plots and effective sample size. Partition point estimates \hat{C}_1 and \hat{C}_2 are calculated by minimizing the VI loss.

The clustering point estimates are displayed in Figure 4(a). There are two birth weight clusters, cluster 1 (with 43 children) and cluster 2 (with 957 children). The maximum birth weight of children in cluster 1 of \hat{C}_1 was 2.183 kg, meaning that all children in cluster 1 would be considered to be premature. 97.7% of the children in this cluster are born pre-term; and that proportion for cluster 2 of \hat{C}_1 is merely 16.1%. In addition, Pearson's chi-squared test rejects the null independence hypothesis between \hat{C}_1 and preterm delivery incidence. Interestingly, \hat{C}_2 has three clusters which do not correspond exactly to the preterm delivery cut-offs. While all 804 full term children were allocated into cluster 2 of \hat{C}_2 , the remaining 196 preterm subjects were split between the three clusters, with 19.9% in cluster 1,

16.3 % in cluster 2, and 63.4% in cluster 3. In fact, all of the subjects allocated to clusters 1 and 3 of \hat{C}_2 were delivered pre-term. Similar to \hat{C}_1 , the chi-squared test for independence between \hat{C}_2 and pre-term delivery rejects the null hypothesis.

	\hat{C}_{21}	\hat{C}_{22}	\hat{C}_{23}	
\hat{C}_{11}	24	2	17	43
\hat{C}_{12}	15	834	108	957
	39	836	125	

Table 4: Contingency table between the clustering point estimates \hat{C}_1 and \hat{C}_2 for the [Longnecker et al. \(2001\)](#) data, along with marginal cluster sizes along the rows and columns.

Along with the clustering point estimates, we find evidence that groups based on birth weight and gestational age are dependent. We quantify the dependence between the partitions using the TARI. The TARI posterior distribution is displayed in Figure 4(b), and has posterior expectation equal to 0.139 and 95% credible interval [0.029, 0.239]. An interesting insight provided by the multiview approach is the ability to infer premature subgroups in each gestational age cluster by inspecting the contingency table for the point estimates (Table 4). Here, we can see, for example, that newborns in \hat{C}_{21} are more likely to be born prematurely than newborns in the other birth weight clusters, and that this probability rapidly diminishes with increasing gestational age. In addition, the separation between the \hat{C}_1 clusters is far larger in \hat{C}_{21} than \hat{C}_{22} and \hat{C}_{23} , indicating that birth weight outcomes are most polarized for earlier births.

7 DISCUSSION AND EXTENSIONS

This article proposes a novel method for Bayesian inference on dependent partitions arising from multiview data. Our approach relies on the PCDP, a nonparametric prior that generates dependent random distributions by centring a DP on a random product measure. The induced $\text{CLIC}(\rho, \gamma_1, \gamma_2)$ distribution has several appealing theoretical properties, such as an independence centered CRP and a closed form expression of the ERI. The probability mass function of the $\text{CLIC}(\rho, \gamma_1, \gamma_2)$ distribution is an MEPPF, a novel generalization of the EPPF that describes the joint distribution of random partitions in terms of their contingency table. In addition, we derive a Gibbs sampler for a finite approximation to the PCDP that can model both uncorrelated and correlated views. Point estimation and uncertainty quantification of the partitions is achieved using standard procedures in the Bayesian clustering literature. A single parameter, ρ , controls perturbations from the independent clustering

model, and the degree of dependence between the partitions is inferred using the Rand index (or the normalized TARI). In simulations and an application to the Longnecker et al. (2001) study, we show that CLIC can capture a wide spectrum of partition dependence.

In comparison to existing methods for Bayesian multiview clustering, our approach does not assume a directional relationship between C_1 and C_2 . Instead, our methodology focuses on describing the joint distribution of (C_1, C_2) using the innovative idea of a cross-partition and, in particular, the MEPPF. The CLIC distribution is one example of a joint partition model that admits an MEPPF, but it is interesting to examine what other joint partition models fall under this framework. Though our construction relies on a hierarchical process for sampling a random measure, it may be the case that an MEPPF can be induced without a data augmentation procedure. This formulation would be especially useful for computation. Modeling ρ as random leads to a fully Bayesian model and additionally leads to vastly improved mixing over setting it equal to a constant, but sampling from the full conditional of ρ requires imputation of the marginal latent probability vectors \tilde{q}_1, \tilde{q}_2 . As in the HDP, the addition of these latent vectors can lead to slow mixing in certain situations. The closed form expression for the distribution of the cross-partition in (14) and the notion of root partitions provide a promising direction for deriving a marginal MCMC sampler, though sampling from $\pi(T_1, T_2 \mid C_1, C_2, \rho, \gamma_1, \gamma_2)$ is not straightforward.

The PCDP can be extended to address several tasks that commonly arise in unsupervised learning. For example, it is often of interest to simultaneously infer a random partition while selecting features that distinguish its clusters (Hancer et al., 2020). A common strategy is to introduce latent discrimination indicators (Tadesse et al., 2005; Kim et al., 2006) $\alpha_{vj_v} \in \{0, 1\}$ for each feature and view. Typically, the indicators are assumed to be independent and identically distributed Bernoulli(ω) random variables. Let $\theta_i^{(1)}$ be the vector of atoms for which $\alpha_{vj_v} = 1$ and $\theta_i^{(0)}$ be the analogous vector for which $\alpha_{vj_v} = 0$; let $\alpha^{(1)}$ and $\alpha^{(0)}$ be similar vectors for the indicators. Inter-view variable selection can be accomplished by modeling $\theta_i^{(0)} \mid \alpha^{(0)} \sim W$, where W is a fixed non-atomic measure, then modeling $\theta_i^{(1)}$ conditional on $\alpha^{(1)}$ with the PCDP. However, it may be the case that we want to adjust for the different views when selecting variables, e.g., when one view is of far higher dimension than the other. To implement this intra-view approach, we concatenate the indicators into $\alpha_v = (\alpha_{vj_v})_{j_v=1}^{d_v}$ for all $v = 1, \dots, V$. We model the members of each α_v as independent Bernoulli(ω_v) variables, where ω_v can be calibrated to match the desired sparsity for the v th view. If $\theta_{vi}^{(0)}$ are the atoms in the v th view for which $\alpha_{vj_v} = 0$, we draw $\theta_{vi}^{(0)} \mid \alpha_v^{(0)} \sim W_v$ for a fixed measure W_v . Alternatively, one could

adapt shrinkage priors developed for variable selection (Yau and Holmes, 2011; Malsiner-Walli et al., 2016) into intra-view and inter-view approaches with the PCDP as the prior on the partitions.

Finally, an intriguing prospect of the PCDP is extending its hierarchical formulation to incorporate graphical dependence structure between the views. For example, for $V = 3$ views, the directed acyclic graph (DAG) for the partitions could be $C_1 \rightarrow C_2 \rightarrow C_3$, in which case $\pi(c_{1i} = k_1, c_{2i} = k_2, c_{3i} = k_3 \mid p) = p_{k_1 k_2}^{(12)} p_{k_3 | k_2}^{(3|2)}$, where $p_{k_v | k_{v-1}}^{(v|v-1)}$ is the conditional probability of the v th label given the $(v - 1)$ th label for clusters k_v and k_{v-1} . In this case, the PCDP could be used to model the pairwise joint distributions between views one and two, and between views two and three. This would allow separate parameters, say ρ_{12} and ρ_{23} , to control concentration towards pairwise independent models. An alternative strategy is to center a random measure on the DAG, i.e. $P \mid \rho, Q \sim \text{DP}(\rho, Q_{12} \times Q_{3|2})$, where Q_{12} is a random joint distribution between the first two views and $Q_{3|2}$ is a random conditional measure between views two and three. When $\rho \rightarrow \infty$, the DAG holds, and hence ρ can be used to test the validity of the graphical model.

ACKNOWLEDGEMENTS

This work was supported by the National Institutes of Health (NIH) under Grants 1R01AI155733, 1R01ES035625, and 5R01ES027498; the United States Office of Naval Research (ONR) Grant N00014-21-1-2510; the European Research Council (ERC) under Grant 856506; and Merck & Co., Inc., through its support for the Merck BARDS Academic Collaboration. The authors thank Amy H. Herring for helpful comments.

REFERENCES

- Aldous, D. J. (1985). Exchangeability and related topics. In P. L. Hennequin (Ed.), *École d'Été de Probabilités de Saint-Flour XIII — 1983*, Berlin, Heidelberg. Springer Berlin Heidelberg.
- Antoniak, C. E. (1974). Mixtures of Dirichlet processes with applications to Bayesian nonparametric problems. *The Annals of Statistics* 2(6), 1152–1174.
- Bailey, J. (2014). Alternative clustering analysis: A review. In *Data Clustering: Algorithms and Applications* (1st ed.), Chapter 21, pp. 535–550. CRC Press.

- Bickel, S. and T. Scheffer (2004). Multi-view clustering. In *Fourth IEEE International Conference on Data Mining*, pp. 19–26.
- Binder, D. A. (1978). Bayesian cluster analysis. *Biometrika* 65(1), 31–38.
- Blackwell, D. and J. B. MacQueen (1973). Ferguson distributions via Pólya urn schemes. *The Annals of Statistics* 1(2), 353–355.
- Camerlenghi, F., A. Lijoi, P. Orbanz, and I. Prünster (2019). Distribution theory for hierarchical processes. *The Annals of Statistics* 47(1), 67–92.
- Camerlenghi, F., A. Lijoi, and I. Prünster (2018). Bayesian nonparametric inference beyond the Gibbs-type framework. *Scandinavian Journal of Statistics* 45(4), 1062–1091.
- Caron, F., M. Davy, and A. Doucet (2007). Generalized Pólya urn for time-varying Dirichlet process mixtures. In *Proceedings of the 23rd Conference on Uncertainty in Artificial Intelligence, UAI 2007*.
- Caron, F., W. Neiswanger, F. Wood, A. Doucet, and M. Davy (2017). Generalized Pólya urn for time-varying Pitman-Yor processes. *Journal of Machine Learning Research* 18(27), 1–32.
- Dahl, D. B., D. J. Johnson, and P. Müller (2022). Search algorithms and loss functions for Bayesian clustering. *Journal of Computational and Graphical Statistics* 31(4), 1189–1201.
- Das, S., Y. Niu, Y. Ni, B. K. Mallick, and D. Pati (2024). Blocked Gibbs sampler for hierarchical Dirichlet processes. *Journal of Computational and Graphical Statistics forthcoming*.
- Dombowsky, A. and D. B. Dunson (2023). Bayesian clustering via fusing of localized densities. *arXiv preprint arXiv:2304.00074*.
- Duan, L. L. (2020). Latent simplex position model: High dimensional multi-view clustering with uncertainty quantification. *The Journal of Machine Learning Research* 21(1), 1411–1435.
- Escobar, M. D. and M. West (1995). Bayesian density estimation and inference using mixtures. *Journal of the American Statistical Association* 90(430), 577–588.
- Fang, U., M. Li, J. Li, L. Gao, T. Jia, and Y. Zhang (2023). A comprehensive survey on multi-view clustering. *IEEE Transactions on Knowledge and Data Engineering* 35(12), 12350–12368.

- Ferguson, T. S. (1973). A Bayesian analysis of some nonparametric problems. *The Annals of Statistics* 1(2), 209–230.
- Franzolini, B., A. Cremaschi, W. van den Boom, and M. De Iorio (2023). Bayesian clustering of multiple zero-inflated outcomes. *Philosophical Transactions of the Royal Society A* 381(2247), 20220145.
- Franzolini, B., M. De Iorio, and J. Eriksson (2023). Conditional partial exchangeability: a probabilistic framework for multi-view clustering. *arXiv preprint arXiv:2307.01152*.
- Fritsch, A. (2012). Package ‘mcclust: Process an MCMC sample of clusterings’.
- Gelman, A., J. B. Carlin, H. S. Stern, D. B. Dunson, A. Vehtari, and D. B. Rubin (2013). *Bayesian Data Analysis*. Chapman and Hall/CRC.
- Gnedin, A. and J. Pitman (2006). Exchangeable Gibbs partitions and Stirling triangles. *Journal of Mathematical Sciences* 138, 5674–5685.
- Hancer, E., B. Xue, and M. Zhang (2020). A survey on feature selection approaches for clustering. *Artificial Intelligence Review* 53(6), 4519–4545.
- Hubert, L. and P. Arabie (1985). Comparing partitions. *Journal of Classification* 2, 193–218.
- Hughes, M. M., R. E. Black, and J. Katz (2017). 2500-g low birth weight cutoff: history and implications for future research and policy. *Maternal and Child Health Journal* 21(2), 283–289.
- Ishwaran, H. and J. S. Rao (2005). Spike and slab variable selection: Frequentist and Bayesian strategies. *The Annals of Statistics* 33(2), 730–773.
- Ishwaran, H. and M. Zarepour (2002). Exact and approximate sum representations for the Dirichlet process. *Canadian Journal of Statistics* 30(2), 269–283.
- James, L. F., A. Lijoi, and I. Prünster (2009). Posterior analysis for normalized random measures with independent increments. *Scandinavian Journal of Statistics* 36(1), 76–97.
- Kass, R. E. and A. E. Raftery (1995). Bayes factors. *Journal of the American Statistical Association* 90(430), 773–795.

- Kim, S., M. G. Tadesse, and M. Vannucci (2006). Variable selection in clustering via Dirichlet process mixture models. *Biometrika* 93(4), 877–893.
- Lee, J., P. Müller, Y. Zhu, and Y. Ji (2016). *A Nonparametric Bayesian Model for Nested Clustering*, pp. 129–141. New York, NY: Springer New York.
- Leisch, F. (2004). Flexmix: A general framework for finite mixture models and latent class regression in R. *Journal of Statistical Software* 11(8), 1–18.
- Lijoi, A., I. Prünster, and T. Rigon (2023). Finite-dimensional discrete random structures and Bayesian clustering. *Journal of the American Statistical Association* forthcoming.
- Lock, E. F. and D. B. Dunson (2013). Bayesian consensus clustering. *Bioinformatics* 29(20), 2610–2616.
- Loftin, R. W., M. Habli, C. C. Snyder, C. M. Cormier, D. F. Lewis, and E. A. DeFranco (2010). Late preterm birth. *Reviews in Obstetrics and Gynecology* 3(1), 10–19.
- Longnecker, M. P., M. A. Klebanoff, H. Zhou, and J. W. Brock (2001). Association between maternal serum concentration of the DDT metabolite DDE and preterm and small-for-gestational-age babies at birth. *The Lancet* 358(9276), 110–114.
- Lu, Z. and W. Lou (2022). Bayesian consensus clustering for multivariate longitudinal data. *Statistics in Medicine* 41(1), 108–127.
- Malsiner-Walli, G., S. Frühwirth-Schnatter, and B. Grün (2016). Model-based clustering based on sparse finite Gaussian mixtures. *Statistics and Computing* 26(1), 303–324.
- Meilă, M. (2007). Comparing clusterings—an information based distance. *Journal of Multivariate Analysis* 98(5), 873–895.
- Miller, J. W. and D. B. Dunson (2019). Robust Bayesian inference via coarsening. *Journal of the American Statistical Association* 114(527), 1113–1125.
- Mitchell, T. J. and J. J. Beauchamp (1988). Bayesian variable selection in linear regression. *Journal of the American Statistical Association* 83(404), 1023–1032.

- Niswander, K. R. and M. Gordon (1972). *The Women and Their Pregnancies: The Collaborative Perinatal Study of the National Institute of Neurological Diseases and Stroke*, Volume 73. National Institute of Health.
- Özçag, E., I. Ege, H. Gürçay, and B. Jolevska-Tuneska (2008). On partial derivatives of the incomplete beta function. *Applied Mathematics Letters* 21(7), 675–681.
- Page, G. L., F. A. Quintana, and D. B. Dahl (2022). Dependent modeling of temporal sequences of random partitions. *Journal of Computational and Graphical Statistics* 31(2), 614–627.
- Paisley, J., C. Wang, D. M. Blei, and M. I. Jordan (2014). Nested hierarchical Dirichlet processes. *IEEE Transactions on Pattern Analysis and Machine Intelligence* 37(2), 256–270.
- Pitman, J. (2002). Combinatorial stochastic processes. Technical Report 621, Department of Statistics, UC Berkeley. Notes for Saint Flour Summer School.
- Rand, W. M. (1971). Objective criteria for the evaluation of clustering methods. *Journal of the American Statistical Association* 66(336), 846–850.
- Rappoport, N. and R. Shamir (2018). Multi-omic and multi-view clustering algorithms: review and cancer benchmark. *Nucleic Acids Research* 46(20), 10546–10562.
- Ren, L., D. B. Dunson, and L. Carin (2008). The dynamic hierarchical Dirichlet process. In *Proceedings of the 25th International Conference on Machine Learning*, pp. 824–831.
- Resnick, S. (2001). *A Probability Path*. Birkhäuser.
- Ritter, C. and M. A. Tanner (1992). Facilitating the Gibbs sampler: the Gibbs stopper and the griddy-Gibbs sampler. *Journal of the American Statistical Association* 87(419), 861–868.
- Rodriguez, A., D. B. Dunson, and A. E. Gelfand (2008). The nested Dirichlet process. *Journal of the American Statistical Association* 103(483), 1131–1154.
- Schlaudecker, E. P., F. M. Munoz, A. Bardají, N. S. Boghossian, A. Khalil, H. Mousa, M. Nesin, M. I. Nisar, V. Pool, H. M. Spiegel, et al. (2017). Small for gestational age: Case definition & guidelines for data collection, analysis, and presentation of maternal immunisation safety data. *Vaccine* 35(48), 6518–6528.

- Scrucca, L., C. Fraley, T. B. Murphy, and A. E. Raftery (2023). *Model-Based Clustering, Classification, and Density Estimation Using mclust in R*. Chapman and Hall/CRC.
- Sethuraman, J. (1994). A constructive definition of Dirichlet priors. *Statistica Sinica* 4(2), 639–650.
- Tadesse, M. G., N. Sha, and M. Vannucci (2005). Bayesian variable selection in clustering high-dimensional data. *Journal of the American Statistical Association* 100(470), 602–617.
- Tang, J. and A. Gupta (1984). On the distribution of the product of independent Beta random variables. *Statistics & Probability Letters* 2(3), 165–168.
- Teh, Y., M. Jordan, M. Beal, and D. Blei (2006). Hierarchical Dirichlet processes. *Journal of the American Statistical Association* 101(476), 1566–1581.
- Teh, Y. W. and M. I. Jordan (2010). Hierarchical Bayesian nonparametric models with applications. In *Bayesian Nonparametrics*, Volume 1, pp. 158–207. Cambridge University Press.
- Wade, S. (2015). Package ‘mclust. ext’.
- Wade, S., D. B. Dunson, S. Petrone, and L. Trippa (2014). Improving prediction from Dirichlet process mixtures via enrichment. *The Journal of Machine Learning Research* 15(1), 1041–1071.
- Wade, S. and Z. Ghahramani (2018). Bayesian cluster analysis: Point estimation and credible balls (with discussion). *Bayesian Analysis* 13(2), 559–626.
- Wade, S., S. Mongelluzzo, and S. Petrone (2011). An enriched conjugate prior for Bayesian nonparametric inference. *Bayesian Analysis* 6(3), 359–385.
- Wei, S., J. Wang, G. Yu, C. Domeniconi, and X. Zhang (2020). Multi-view multiple clusterings using deep matrix factorization. In *Proceedings of the AAAI Conference on Artificial Intelligence*, Volume 34, pp. 6348–6355.
- Wilks, S. S. (1932). Certain generalizations in the analysis of variance. *Biometrika* 24(3/4), 471–494.
- Yao, S., G. Yu, J. Wang, C. Domeniconi, and X. Zhang (2019). Multi-view multiple clustering. In *Proceedings of the 28th International Joint Conference on Artificial Intelligence, IJCAI’19*, pp. 4121–4127. AAAI Press.

Yau, C. and C. Holmes (2011). Hierarchical Bayesian nonparametric mixture models for clustering with variable relevance determination. *Bayesian Analysis* 6(2), 329–352.

Yu, G., L. Ren, J. Wang, C. Domeniconi, and X. Zhang (2024). Multiple clusterings: Recent advances and perspectives. *Computer Science Review* 52, 100621.

Zito, A., T. Rigon, and D. B. Dunson (2023). Bayesian nonparametric modeling of latent partitions via Stirling-gamma priors. *arXiv preprint arXiv:2306.02360*.

SUPPLEMENTARY MATERIAL

Proofs of all results and extended details on simulations and the application to the CPP data are available in the Supplementary Material. Code for the simulations and application is available at <https://github.com/adombowsky/clic>.

A PROOFS AND ADDITIONAL RESULTS

A.1 IDENTIFIABILITY OF CONCENTRATION PARAMETERS

In this section, we verify that the key hyperparameters $(\rho, \gamma_1, \gamma_2)$ are identifiable in the joint prior for (P, Q_1, Q_2) . Let S_{v1}, \dots, S_{vm_v} be a partition of Θ_v and assume that $H_v(S_{vk_v}) > 0$ for all $k_v = 1, \dots, m_v$. By definition of the DP,

$$(Q_v(S_{v1}), \dots, Q_v(S_{vm_v})) \mid \gamma_v \sim \text{Dir}(\gamma_v H_v(S_{v1}), \dots, \gamma_v H_v(S_{vm_v})). \quad (25)$$

This Dirichlet distribution is a one parameter exponential family, with sufficient statistic $\sum_{u_v=1}^{m_v} H_v(S_{vm_v}) \log Q_v(S_{v1})$ and canonical parameter γ_v . Hence, γ_v is identifiable in the prior for Q_v . Moreover, let S_1, \dots, S_m be a partition of $\Theta = \Theta_1 \times \Theta_2$ and Q be *any probability measure* on Θ with $Q(S_k) > 0$ for all $k = 1, \dots, m$. By definition,

$$(P(S_1), \dots, P(S_m)) \mid \rho, Q \sim \text{Dir}(\rho Q(S_1), \dots, \rho Q(S_m)), \quad (26)$$

and so by a similar argument for Q_v , ρ is identifiable in the prior for $P \mid Q$.

Next, let $\{\{S_{v1}, \dots, S_{vm_v}\}_{v=1,2}\}$ be partitions of Θ_1 and Θ_2 with $H_v(S_{vk_v}) > 0$ for all k_v and v , and create a partition of Θ with $\{S_{1k_1} \times S_{2k_2}\}_{u_1, u_2}$. We now define a joint prior density over (a) a

measure of the joint partition $\{S_{1u_1} \times S_{2u_2}\}_{u_1, u_2}$, (b) a measure of the marginal partition along Θ_1 , and (c) a measure of the marginal partition along Θ_2 . Let p belong to the $m_1 m_2 - 1$ simplex, q_1 belong to the $m_1 - 1$ simplex, and q_2 belong to the $m_2 - 1$ simplex. The notation $\pi(p \mid \rho, q_1, q_2)$ denotes the density function of (26) and $\pi(q_v \mid \gamma_v)$ denotes the density function of (25) for $v = 1, 2$. We occasionally collect all hyperparameters into the vector $\varphi = (\rho, \gamma_1, \gamma_2)$. Hence, $\pi(p, q_1, q_2 \mid \varphi) = \pi(p \mid \rho, q_1, q_2)\pi(q_1 \mid \gamma_1)\pi(q_2 \mid \gamma_2)$.

Suppose that $\pi(p, q_1, q_2 \mid \varphi) = \pi(p, q_1, q_2 \mid \varphi')$ for all p, q_1, q_2 in their respective supports. This is equivalent to

$$\forall p, q_1, q_2, \quad \pi(p \mid \rho, q_1, q_2)\pi(q_1 \mid \gamma_1)\pi(q_2 \mid \gamma_2) = \pi(p \mid \rho', q_1, q_2)\pi(q_1 \mid \gamma'_1)\pi(q_2 \mid \gamma'_2). \quad (27)$$

Thus, for any q_1, q_2 ,

$$\begin{aligned} \int \pi(p \mid \rho, q_1, q_2)\pi(q_1 \mid \gamma_1)\pi(q_2 \mid \gamma_2)dp &= \int \pi(p \mid \rho', q_1, q_2)\pi(q_1 \mid \gamma'_1)\pi(q_2 \mid \gamma'_2)dp \\ \implies \forall q_1, q_2, \quad \pi(q_1 \mid \gamma_1)\pi(q_2 \mid \gamma_2) &= \pi(q_1 \mid \gamma'_1)\pi(q_2 \mid \gamma'_2). \end{aligned} \quad (28)$$

Similarly, for any q_1 ,

$$\begin{aligned} \int \pi(q_1 \mid \gamma_1)\pi(q_2 \mid \gamma_2)dq_2 &= \int \pi(q_1 \mid \gamma'_1)\pi(q_2 \mid \gamma'_2)dq_2 \\ \implies \forall q_1, \quad \pi(q_1 \mid \gamma_1) &= \pi(q_1 \mid \gamma'_1). \end{aligned} \quad (29)$$

As γ_1 is identifiable, (29) implies $\gamma_1 = \gamma'_1$. (28) simplifies to $\pi(q_2 \mid \gamma_2) = \pi(q_2 \mid \gamma'_2)$ for all q_2 and so $\gamma_2 = \gamma'_2$. By a similar argument for (27), $\rho = \rho'$.

A.2 PROOF OF THEOREM 1

Proof. In the independence centered CRP, the customer can either choose an entrée and table from the contingency table, or they can make their choices independently. Denote $r^{(i)}$ to be the number of times that customers $1, \dots, i - 1$ made independent choices. To make the CRP metaphor more concrete, we introduce the notion of pseudo-unique values $\vartheta_1^*, \dots, \vartheta_{r^{(i)}}^*$ and view-specific pseudo-unique values $\vartheta_{v1}^*, \dots, \vartheta_{vr^{(i)}}^*$, defined by $\vartheta_l^* \mid Q \sim Q$ for all $l = 1, \dots, r^{(i)}$.

Recall the stick-breaking process representation of the DP ([Sethuraman, 1994](#)),

$$Q_v = \sum_{k_v=1}^{\infty} q_{vk_v} \delta_{\vartheta_{vk_v}^*}, \quad q_{vk_v} = \beta_{vk_v} \prod_{m_v < k_v} (1 - \beta_{vm_v}), \quad \beta_{vk_v} \sim \text{Beta}(1, \gamma_v), \quad \theta_{vk_v}^* \sim H. \quad (30)$$

Since the Q_v are discrete and Q is the product measure, we have that for any $\theta = (\theta_1, \dots, \theta_V) \in \Theta$,

$$\begin{aligned} Q(\theta) &\stackrel{a.s.}{=} \sum_{k_1=1}^{\infty} \cdots \sum_{k_V=1}^{\infty} \left\{ \prod_{v=1}^V q_{vk_v} \right\} \delta_{\theta_v^*}(\theta) \\ &\stackrel{a.s.}{=} \sum_{k_1=1}^{\infty} \cdots \sum_{k_V=1}^{\infty} \prod_{v=1}^V q_{vk_v} \delta_{\theta_{vk_v}^*}(\theta_v) \stackrel{a.s.}{=} \prod_{v=1}^V \left\{ \sum_{k_v=1}^{\infty} q_{vk_v} \delta_{\theta_{vk_v}^*} \right\} = \prod_{v=1}^V Q_v(\theta_v), \end{aligned} \quad (31)$$

by Fubini's theorem. Hence, by independence we have that

$$\mathbb{E}[Q \mid \vartheta_1^*, \dots, \vartheta_{r^{(i)}}^*] = \prod_{v=1}^V \mathbb{E}[Q_v \mid \vartheta_1^*, \dots, \vartheta_{r^{(i)}}^*] = \prod_{v=1}^V \mathbb{E}[Q_v \mid \vartheta_{v1}^*, \dots, \vartheta_{v r^{(i)}}^*].$$

Observe that each term in the product measure above is just the posterior expectation of a Dirichlet process (see, for example [Gelman et al. \(2013\)](#)),

$$\mathbb{E}[Q_v \mid \vartheta_{v1}^*, \dots, \vartheta_{v r^{(i)}}^*] = \frac{1}{\gamma_v + r^{(i)}} \sum_{l_v=1}^{r^{(i)}} \delta_{\vartheta_{vl_v}^*} + \frac{\gamma_v}{\gamma_v + r^{(i)}} H_v. \quad (32)$$

Under this sampling scheme, we can now see that, provided H_v is non-atomic, there will be ties amongst the pseudo-unique values $\vartheta_{v1}^*, \dots, \vartheta_{v r^{(i)}}^*$ into unique values $\theta_{v1}^*, \dots, \theta_{v K_v^{(i)}}^*$ where $K_v^{(i)} \leq r^{(i)}$. We then denote $r_{vk_v} = \sum_{l_v=1}^{r^{(i)}} \mathbf{1}(\vartheta_{vl_v}^* = \theta_{vk_v}^*)$ for all $k_v = 1, \dots, K_v$, which counts the number of times that the first $i-1$ customers chose an occupied table or already served dish given that they made the choices independently. This also implies that $\sum_{k_v=1}^{K_v^{(i)}} r_{vk_v} = r^{(i)}$. We can then rewrite (32) as

$$\mathbb{E}[Q_v \mid \theta_{v1}^*, \dots, \theta_{v K_v^{(i)}}^*] = \frac{1}{\gamma_v + r^{(i)}} \sum_{k_v=1}^{K_v^{(i)}} r_{vk_v} \delta_{\theta_{vk_v}^*} + \frac{\gamma_v}{\gamma_v + r^{(i)}} H_v. \quad (33)$$

Now, we address the predictive distribution of θ_i . Conditional on Q and $\vartheta_1^*, \dots, \vartheta_{r^{(i)}}^*$, the Blackwell-MacQueen urn scheme ([Blackwell and MacQueen, 1973](#)) holds (e.g., as in the HDP in [Teh et al. \(2006\)](#)), resulting in

$$\theta_i \mid \vartheta_1^*, \dots, \vartheta_{r^{(i)}}^*, \rho, Q \sim \frac{1}{\rho + i - 1} \sum_{l_1, \dots, l_V} w_{l_1 \dots l_V} \delta_{(\vartheta_{1l_1}^*, \dots, \vartheta_{Vl_V}^*)} + \frac{\rho}{\rho + i - 1} Q, \quad (34)$$

where the sum is taken over $l_1 \in [r^{(i)}], \dots, l_V \in [r^{(i)}]$ and $w_{l_1 \dots l_V} = \sum_{j=1}^{i-1} \mathbf{1}(\theta_{j1} = \vartheta_{l_1}^*, \dots, \theta_{jV} = \vartheta_{l_V}^*)$, and $\sum_{k_1, \dots, k_v} w_{k_1 \dots k_v} = i - 1$. As mentioned previously, there are groups amongst the pseudo-unique values, which we count with

$$n_{k_1 \dots k_v} = \sum_{l_1, \dots, l_V} \mathbf{1}(\vartheta_{l_1} = \theta_{1k_1}^*, \dots, \vartheta_{l_V} = \theta_{V k_v}^*) w_{l_1 \dots l_V},$$

which correspond to the entries in the contingency array. Denote $\mathbf{r}_v = (r_{v1}, \dots, r_{vK_v^{(i)}})$ for all $v = 1, \dots, V$. Using (32) and (33), we can marginalize out Q from (34) to obtain

$$\theta_i | \theta^{(i)}, \rho \sim \sum_{k_1, \dots, k_V} \frac{n_{k_1 \dots k_V}}{\rho + i - 1} \delta_{(\theta_{1k_1}^*, \dots, \theta_{V k_V}^*)} + \frac{\rho}{\rho + i - 1} \times_{v=1}^V \left\{ \sum_{k_v=1}^{K_v^{(i)}} \frac{r_{v k_v}}{\gamma_v + r^{(i)}} \delta_{\theta_{v k_v}^*} + \frac{\gamma_v}{\gamma_v + r^{(i)}} H_v \right\}.$$

□

A.3 PROOF OF PROPOSITION 1

Proof. First, we show (i). Let $\epsilon > 0$ and assume that ρ is fixed, i.e., we will show all results by conditioning on ρ , though we will not use the conditional notation. Using Markov's inequality,

$$\pi(|P(S) - Q(S)| > \epsilon | Q) \leq \frac{\text{Var}[P(S) | Q]}{\epsilon^2} = \frac{Q(S) \{1 - Q(S)\}}{\epsilon^2(\rho + 1)} \leq \frac{1}{4\epsilon^2(\rho + 1)}. \quad (35)$$

Next, we take the expectation of both sides of (35) with respect to the prior for Q . Since the right hand side does not depend on Q , we have that $\pi(|P(S) - Q(S)| > \epsilon) \leq 1/(4\epsilon^2(\rho + 1))$ for any fixed value of $\rho > 0$. If we construct a countable sequence of ρ values with an infinite limit, this shows that for any $\epsilon > 0$, $\lim_{\rho \rightarrow \infty} \pi(|P(S) - Q(S)| > \epsilon) = 0$.

For (ii), observe that $Q_v(S_v) \xrightarrow{p} H_v(S_v)$ as $\gamma_v \rightarrow \infty$ for $v = 1, 2$. Fix $\lambda \in [0, 1]$ to be any continuity point for the CDF of $P(S)$. Recall that $P(S) | \rho, Q(S) \sim \text{Beta}(\rho Q(S), \rho Q(S^c))$. Since the partial derivatives of the incomplete beta function exist for all shape parameters (Özçag et al., 2008), the continuous mapping theorem implies convergence of the CDFs in prior probability,

$$\Pi(\lambda | Q_1(S_1), Q_2(S_2)) \xrightarrow{p} \Pi(\lambda | H_1(S_1), H_2(S_2)). \quad (36)$$

Using the dominated convergence theorem applied to $\pi\{P(S) \leq \lambda | Q_1(S_1), Q_2(S_2)\}$, we get that $P(S) \xrightarrow{d} P_0(S)$. □

A.4 PROOF OF PROPOSITION 2

Proof. Ishwaran and Zarepour (2002) shows that as $L_v \rightarrow \infty$, $\int h_v(\theta_v) d\tilde{Q}_v(\theta_v) \xrightarrow{d} \int h_v(\theta_v) dQ_v(\theta_v)$ for all measurable h_v . Using Fubini's theorem, we have that

$$\int \int h(\theta) d\tilde{Q}(\theta) = \int h_1(\theta_1) d\tilde{Q}_1(\theta_1) \int h_2(\theta_2) d\tilde{Q}_2(\theta_2). \quad (37)$$

Recall that $\tilde{Q}_1 \perp \tilde{Q}_2$, $\tilde{Q}_1 \perp Q_2$, $\tilde{Q}_2 \perp Q_1$, and $Q_1 \perp Q_2$. Therefore, by the continuous mapping theorem,

$$\int h_1(\theta_1) d\tilde{Q}_1(\theta_1) \int h_2(\theta_2) d\tilde{Q}_2(\theta_2) \xrightarrow{d} \int h_1(\theta_1) dQ_1(\theta_1) \int h_2(\theta_2) dQ_2(\theta_2),$$

and the result follows by applying Fubini's theorem to the right hand side of the above. □

A.5 PROOF OF THEOREM 2

Proof. The result largely follows by adapting the proof of Theorem 1 in Camerlenghi et al. (2018), which derives the EPPF resulting from an HDP. Let $\theta_1 \neq \dots \neq \theta_K$ be fixed, where $\theta_k = (\theta_{1k}, \theta_{2k})$. Consider the function

$$M_n(d\theta_1, \dots, d\theta_K) = \mathbb{E} \left\{ \prod_{k_1, k_2} P^{n_{k_1 k_2}}(d(\theta_{1k_1}, \theta_{2k_2})) \right\}.$$

The connection between $M_n(d\theta_1, \dots, d\theta_K)$ and $\Pi(C_1, C_2 \mid \rho, \gamma_1, \gamma_2)$ is that the MEPPF is equal to the integral of the above with respect to $\theta_1 \neq \dots \neq \theta_K$. Suppose now that we create an ϵ -rectangle around each θ_k , denoted by $B_{k_1, k_2, \epsilon} = B_{1k_1, \epsilon} \times B_{2k_2, \epsilon}$, where $B_{vk_v, \epsilon} = \{x \in \Theta_v : \|\theta_{vk_v} - x\| < \epsilon\}$, and ϵ is small enough so that $B_{k_1, k_2, \epsilon}$ are disjoint for all k_1, k_2 . It follows then that

$$\begin{aligned} M_n \left(\times_{k_1, k_2} B_{k_1, k_2, \epsilon} \right) &= \mathbb{E} \left\{ \prod_{k_1, k_2} P^{n_{k_1 k_2}}(B_{k_1, k_2, \epsilon}) \mid Q_1, Q_2 \right\} \\ &= \frac{1}{\Gamma(n)} \mathbb{E} \int_0^\infty u^{n-1} e^{-\rho \Psi(u) Q(\Theta_\epsilon^c)} \prod_{k_1, k_2} \left\{ (-1)^{n_{k_1 k_2}} \frac{d^{n_{k_2 k_2}}}{du^{n_{k_1 k_2}}} e^{-\rho \Psi(u) Q(B_{k_1, k_2, \epsilon})} \right\} du, \end{aligned}$$

where $\Theta_\epsilon^c = \Theta \setminus \bigcup_{k_1, k_2} B_{k_1, k_2, \epsilon}$ and for any $u > 0$, $\Psi(u) = \int_0^\infty \{1 - e^{-u\nu}\} \nu^{-1} e^{-\nu} d\nu$. By applying equation (A2) in [Camerlenghi et al. \(2018\)](#), we have that

$$\begin{aligned} & M_n \left(\times_{k_1, k_2} B_{k_1, k_2, \epsilon} \right) \\ &= \frac{1}{\Gamma(n)} \int_0^\infty u^{n-1} e^{-\rho\Psi(u)} \sum_{r \in \mathcal{R}} \rho^r \left(\mathbb{E} \prod_{k_1, k_2} Q^{r_{k_1 k_2}}(B_{k_1, k_2, \epsilon}) \xi_{n_{k_1 k_2}, r_{k_1 k_2}}(u) \right) du, \end{aligned} \quad (38)$$

where for any two integers m, n ,

$$\xi_{n, m}(u) = \frac{1}{m!} \sum_{w \in W} \binom{n}{w_1 \cdots w_m} \frac{\prod_{l=1}^m \Gamma(w_l)}{(u+1)^n},$$

and the summation is over $W = \{w = (w_1, \dots, w_m) : w_l \in \mathbb{N}, \sum_{l=1}^m w_l = n\}$. Observe that, under the assumption that $\mathcal{S}_1, \mathcal{S}_2$ are Borel algebras, with probability equal to 1,

$$\begin{aligned} \prod_{k_1, k_2} Q^{r_{k_1 k_2}}(B_{k_1, k_2, \epsilon}) &= \prod_{k_1, k_2} \left\{ Q_1^{r_{k_1 k_2}}(B_{1k_1, \epsilon}) Q_2^{r_{k_1, k_2}}(B_{2k_2, \epsilon}) \right\} \\ &= \prod_{k_1} Q_1^{r_{1k_1}}(B_{1k_1, \epsilon}) \prod_{k_2} Q_2^{r_{2k_2}}(B_{2k_2, \epsilon}). \end{aligned}$$

By independence of Q_1 and Q_2 ,

$$\mathbb{E} \prod_{k_1, k_2} Q^{r_{k_1 k_2}}(B_{k_1, k_2, \epsilon}) = \mathbb{E} \prod_{k_1} Q_1^{r_{1k_1}}(B_{1k_1, \epsilon}) \mathbb{E} \prod_{k_2} Q_2^{r_{2k_2}}(B_{2k_2, \epsilon}).$$

Returning to (38), we have that

$$\begin{aligned} & M_n \left(\times_{k_1, k_2} B_{k_1, k_2, \epsilon} \right) = \\ & \frac{1}{\Gamma(n)} \sum_{r \in \mathcal{R}} M_{r_1} \left(\times_{k_1} B_{1k_1, \epsilon} \right) M_{r_2} \left(\times_{k_2} B_{2k_2, \epsilon} \right) \rho^r \int_0^\infty u^{n-1} e^{-\rho\Psi(u)} \left\{ \prod_{k_1, k_2} \xi_{n_{k_1 k_2}, r_{k_1 k_2}}(u) \right\} du, \end{aligned}$$

where $M_{r_v}(d\theta_{v1}, \dots, \theta_{vK_v}) = \mathbb{E} \prod_{k_v} Q_v^{r_{vk_v}}(d\theta_{vk_v})$ for $v = 1, 2$. Using Proposition 3 of [James et al. \(2009\)](#), we have that for $v = 1, 2$,

$$M_{r_v}(d\theta_{v1}, \dots, \theta_{vK_v}) = \left(\prod_{k_v} H_v(d\theta_{vk_v}) \right) \frac{\gamma_v^{K_v}}{(\gamma_v)^{(|r_v|)}} \prod_{k_1} (r_{vk_v} - 1)!,$$

where $|r_v| = \sum_{k_v=1}^{K_v} r_{vk_v} = r$ for $v = 1, 2$. The MEPPF is obtained by taking $\epsilon \rightarrow 0$, then applying Example 1 in [Camerlenghi et al. \(2018\)](#). \square

A.6 PROOF OF THEOREM 3

Proof. We express the PCDP in terms of a stick-breaking representation using the technique in [Teh et al. \(2006\)](#) for the HDP stick-breaking decomposition. We first begin by sampling the marginals Q_v . We write $Q_v = \sum_{k_v=1}^{\infty} q_{vk_v} \delta_{\theta_{vk_v}^*}$, where $\theta_{vk_v}^* \sim H_v$, $q_{vk_v} = \beta_{vk_v} \prod_{m_v < k_v} (1 - \beta_{vm_v})$, and $\beta_{vk_v} \sim \text{Beta}(1, \gamma_v)$. We collect the individual weights of each Q_v into the infinite-dimensional probability vectors $q_v = (q_{vk_v})_{k_v=1}^{\infty}$. Observe that the support of P is comprised of the Cartesian product of the supports of Q_1, Q_2 . This implies that we can rewrite P as

$$P = \sum_{k_1=1}^{\infty} \sum_{k_2=1}^{\infty} p_{k_1 k_2} \delta_{(\theta_{1k_1}^*, \theta_{2k_2}^*)}, \quad (39)$$

where $0 \leq p_{k_1 k_2} \leq 1$ and $\sum_{k_1=1}^{\infty} \sum_{k_2=1}^{\infty} p_{k_1 k_2} = 1$. We denote $p = (p_{k_1 k_2})_{k_1, k_2}$ to be the matrix of probabilities constructed from the weights in (39). Assuming that H_1, H_2 are non-atomic, the probability matrix is itself a Dirichlet process centered on the product measure of q_1 and q_2 ,

$$p \mid \rho, q \sim \text{DP}(\rho, q); \quad q = q_1 \otimes q_2,$$

where \otimes is the tensor product. Conditional on p ,

$$\mathbb{E}[R(C_1, C_2) \mid p] = \sum_{k_1=1}^{\infty} \sum_{k_2=1}^{\infty} p_{k_1 k_2}^2 + \sum_{k_1 \neq m_1}^{\infty} \sum_{k_2 \neq m_2}^{\infty} p_{k_1 k_2} p_{m_1 m_2}. \quad (40)$$

Observe that $\mathbb{E}[R(C_1, C_2) \mid p]$ is an infinite sum. However, all terms in the sum are positive and the Rand index is bounded above by 1, so we can exploit the linearity of expectation by invoking Fubini's theorem, which we will implicitly invoke multiple times by using the law of total expectation. By definition, $p_{k_1 k_2} \mid \rho, q \sim \text{Beta}(\rho q_{1k_1} q_{2k_2}, \rho(1 - q_{1k_1} q_{2k_2}))$. This implies

$$\begin{aligned} \mathbb{E}[p_{k_1 k_2}^2 \mid q_{1k_1}, q_{2k_2}] &= \frac{q_{1k_1} q_{2k_2} (1 - q_{1k_1} q_{2k_2})}{\rho + 1} + q_{1k_1}^2 q_{2k_2}^2; \\ \mathbb{E}[q_{k_1 k_2} q_{m_1 m_2} \mid q_{1k_1}, q_{1m_1}, q_{2k_2}, q_{2m_2}] &= \left(1 - \frac{1}{\rho + 1}\right) q_{1k_1} q_{1m_1} q_{2k_2} q_{2m_2}. \end{aligned}$$

Similarly, we have that $q_1 \perp q_2$ and distributed as stick-breaking processes with concentration parameters γ . Calculating the expectation of (40) requires computing the moments of a stick-breaking process. For $k_v > m_v$, these are

$$\begin{aligned}\mathbb{E}[q_{vk_v}] &= \frac{\gamma^{k_v-1}}{(1+\gamma)^{k_v}} \\ \mathbb{E}[q_{vk_v}^2] &= \left\{ \frac{\gamma}{(\gamma+1)^2(\gamma+2)} + \frac{1}{(1+\gamma)^2} \right\} \left\{ \frac{\gamma}{(\gamma+1)^2(\gamma+2)} + \frac{\gamma^2}{(1+\gamma)^2} \right\}^{k_v-1} \\ \mathbb{E}[q_{vk_v}q_{vm_v}] &= \frac{\gamma}{(\gamma+1)^2(\gamma+2)} \left(\frac{\gamma}{\gamma+1} \right)^{k_v-m_v-1} \left\{ \frac{\gamma}{(\gamma+1)^2(\gamma+2)} + \frac{\gamma^2}{(1+\gamma)^2} \right\}^{m_v-1}\end{aligned}$$

By plugging these terms back into (40), we then need to compute the limits of several power series, all of which are geometric. In particular, we have that

$$\sum_{k_v=1}^{\infty} \mathbb{E}[q_{vk_v}] = 1; \quad \sum_{k_v=1}^{\infty} \mathbb{E}[q_{vk_v}^2] = \frac{1}{\gamma+1}; \quad 2 \sum_{m_v=1}^{\infty} \sum_{k_v=m_v+1}^{\infty} \mathbb{E}[q_{vk_v}q_{vm_v}] = \frac{\gamma}{\gamma+1}. \quad (41)$$

Plugging these identities back into (40) shows that

$$\begin{aligned}\tau_{12} &= \frac{1}{\rho+1} + \left(1 - \frac{1}{\rho+1}\right) \left(\frac{1}{(\gamma+1)^2} + \frac{\gamma^2}{(\gamma+1)^2} \right) \\ &= \frac{1}{\rho+1} + \left(1 - \frac{1}{\rho+1}\right) \frac{\gamma^2+1}{(\gamma+1)^2}.\end{aligned}$$

By Corollary 1 in Page et al. (2022), the expected Rand index of two independent $\text{CRP}(\gamma)$ partitions is $(\gamma^2+1)/(\gamma+1)^2$. This shows how ρ shrinks toward independent $\text{CRP}(\gamma)$ partitions. Additionally, increased γ pulls the expected Rand index to one, reflecting the tendency of (C_1, C_2) to concentrate towards a $\text{CRP}(\rho)$ distribution for large γ .

Observe that in the case where $\gamma_1 \neq \gamma_2$, (41) implies that

$$\begin{aligned}\tau_{12} &= \frac{1}{\rho+1} + \left(1 - \frac{1}{\rho+1}\right) \left\{ \frac{1}{(\gamma_1+1)(\gamma_2+1)} + \frac{\gamma_1\gamma_2}{(\gamma_1+1)(\gamma_2+1)} \right\} \\ &= \frac{1}{\rho+1} + \left(1 - \frac{1}{\rho+1}\right) \frac{1+\gamma_1\gamma_2}{(\gamma_1+1)(\gamma_2+1)}.\end{aligned}$$

□

A.7 ERI OF THE FINITE APPROXIMATION

We now return to the finite approximation to the PCDP presented in Section 2, which we use during our simulations and application. As stated in the main article, the ERI under the finite approximation converges to the ERI of the PCDP as the number of components is taken to infinity.

Proposition 3. Let $\tilde{\tau}_{12}$ be the ERI of C_1 and C_2 under the finite approximation to the PCDP in (12). Then $\tilde{\tau}_{12} = \nu + (1 - \nu)\kappa(L_1, L_2)$, where $\kappa(L_1, L_2) \rightarrow (1 + \gamma^2)/(1 + \gamma)^2$ as $L_1, L_2 \rightarrow \infty$.

Proof. Similar to the infinite case, for any probability matrix \tilde{p} , one can show that

$$\mathbb{E}[R(C_1, C_2) \mid \tilde{p}] = \sum_{k_1=1}^{L_1} \sum_{k_2=1}^{L_2} \tilde{p}_{k_1 k_2}^2 + \sum_{k_1 \neq m_1} \sum_{k_2 \neq m_2} \tilde{p}_{k_1 k_2} \tilde{p}_{m_1 m_2}.$$

If $\tilde{p} = \tilde{p}_1 \otimes \tilde{p}_2$, with $\tilde{p}_1 \sim \text{Dir}(\gamma/L_1, \dots, \gamma/L_1)$, $\tilde{p}_2 \sim \text{Dir}(\gamma/L_2, \dots, \gamma/L_2)$, and $\tilde{p}_1 \perp \tilde{p}_2$, then we have that

$$\begin{aligned} \mathbb{E}[\tilde{p}_{k_1 k_2}^2] &= \mathbb{E}[\tilde{p}_{1 k_1}^2] \mathbb{E}[\tilde{p}_{2 k_2}^2] = \left\{ \frac{(1/L_1)(1 - 1/L_1)}{\gamma + 1} + \frac{1}{L_1^2} \right\} \left\{ \frac{(1/L_2)(1 - 1/L_2)}{\gamma + 1} + \frac{1}{L_2^2} \right\} \\ \mathbb{E}[\tilde{p}_{k_1 k_2} \tilde{p}_{m_1 m_2}] &= \mathbb{E}[\tilde{p}_{1 k_1} \tilde{p}_{1 m_1}] \mathbb{E}[\tilde{p}_{2 k_2} \tilde{p}_{2 m_2}] = \frac{\gamma^2}{(\gamma + 1)^2} \frac{1}{L_1^2 L_2^2}. \end{aligned}$$

So for $C_1 \perp C_2$, with both distributed as symmetric Dirichlet-multinomial partitions,

$$\begin{aligned} \mathbb{E}[R(C_1, C_2) \mid \gamma] &= \kappa(L_1, L_2) \\ &= \left(\frac{1 - 1/L_1}{\gamma + 1} + \frac{1}{L_1^2} \right) \left(\frac{1 - 1/L_2}{\gamma + 1} + \frac{1}{L_2^2} \right) + \frac{(1 - 1/L_1)(1 - 1/L_2)\gamma^2}{(\gamma + 1)^2}. \end{aligned}$$

Note that $\lim_{L_1, L_2 \rightarrow \infty} \kappa(L_1, L_2) = (1 + \gamma^2)/(1 + \gamma)^2$, the ERI for two independent CRP(γ) partitions.

Next, assume (C_1, C_2) is distributed as partitions induced by the finite approximation to the PCDP in (12) with $\gamma_1 = \gamma_2 = \gamma$. Conditional on \tilde{q}_1, \tilde{q}_2 ,

$$\begin{aligned} \mathbb{E}[\tilde{p}_{k_1 k_2}^2 \mid \tilde{q}_{1 k_1}, \tilde{q}_{2 k_2}] &= \frac{\tilde{q}_{1 k_1} \tilde{q}_{2 k_2} (1 - \tilde{q}_{1 k_1} \tilde{q}_{2 k_2})}{\rho + 1} + \tilde{q}_{1 k_1}^2 \tilde{q}_{2 k_2}^2 \\ \mathbb{E}[\tilde{p}_{k_1 k_2} \tilde{p}_{m_1 m_2} \mid \tilde{q}_{1 k_1}, \tilde{q}_{2 k_2}] &= \left(1 - \frac{1}{\rho + 1} \right) \tilde{q}_{1 k_1} \tilde{q}_{2 k_2} \tilde{q}_{1 m_1} \tilde{q}_{2 m_2}. \end{aligned}$$

Set $\nu = 1/(\rho + 1)$. Recall that $\tilde{q}_v \sim \text{Dir}(\gamma/L_v, \dots, \gamma/L_v)$ for $v = 1, 2$. Hence,

$$\mathbb{E}[\tilde{p}_{k_1 k_2}^2] = \frac{\nu}{L_1 L_2} + (1 - \nu) \left\{ \frac{(1/L_1)(1 - 1/L_1)}{\gamma + 1} + \frac{1}{L_1^2} \right\} \left\{ \frac{(1/L_2)(1 - 1/L_2)}{\gamma + 1} + \frac{1}{L_2^2} \right\}; \quad (42)$$

$$\mathbb{E}[\tilde{p}_{k_1 k_2} \tilde{p}_{m_1 m_2}] = (1 - \nu) \frac{\gamma^2}{L_1^2 L_2^2 (\gamma + 1)^2}. \quad (43)$$

The result follows by multiplying (42) and (43) by $L_1 L_2$ and $L_1 L_2 (L_1 - 1)(L_2 - 1)$, respectively, then summing them together. \square

Remark 1. Let $L_1 = L_2 = L$. Then $|\tau_{12} - \tilde{\tau}_{12}| \propto \{(\gamma/L) - \gamma + 1\}/L$, where proportionality is in terms of L . For example, if $\gamma = 1$, then $|\tau_{12} - \tilde{\tau}_{12}| \propto 1/L^2$.

Proof. Using equations (42) and (43), we can see that

$$\begin{aligned} & \tilde{\tau}_{12} - \tau_{12} \\ &= (1 - \nu) \left\{ \left(\frac{1 - 1/L}{\gamma + 1} + 1/L \right)^2 - \frac{1}{(\gamma + 1)^2} + ((1 - 1/L)^2 - 1) \frac{\gamma^2}{(\gamma + 1)^2} \right\} \\ &= (1 - \nu) \left\{ (1/L^2 - 2/L) \frac{\gamma^2 + 1}{(\gamma + 1)^2} + \frac{(2/L)(1 - 1/L)}{\gamma + 1} + 1/L^2 \right\} \\ &= \frac{2\gamma(1 - \nu)}{L(\gamma + 1)^2} \left\{ \frac{\gamma}{L} - \gamma + 1 \right\}. \end{aligned}$$

\square

B ADDITIONAL DETAILS ON SIMULATIONS

Code for all simulations and the application to the CPP data is available in the [CLIC Github repository](#). For the simulations in Section 4, we set $\theta_0 = 0$ and $\sigma_0 = 1$. For the priors on σ_v^2 , we use the Gamma(1, 1) distribution, and for the number of components we set $L_v = 5$. The t-HDP of [Franzolini et al. \(2023\)](#) is implemented using code from the Github page of the first author, where the base measures are taken to be $\mathcal{N} - \mathcal{IG}(0, 1, 1, 1)$, the DP concentration parameters are both set equal to 1, and the number of components are both set to be 5. The EM algorithm is implemented with the R package `mclust` ([Scrucca et al., 2023](#)). The clustering point estimates are computed with the R package `mcclust` ([Fritsch, 2012](#)) and `mcclust.ext` ([Wade, 2015](#)) using the `min.VI()` function, which we also use in the application to the [Longnecker et al. \(2001\)](#) data in Section 6.

B.1 JOINT AND CONDITIONAL SAMPLERS FOR THE LABELS

A key step in the Gibbs sampler is imputing (c_{1i}, c_{2i}) for each object. There are multiple strategies for sampling the labels a priori given the clustering formations C_v^{-i} , where C_v^{-i} is the v th partition with object i removed. In the *joint sampler*, we sample (c_{1i}, c_{2i}) using a matrix multinomial given by

$$\pi(c_{1i} = k_1, c_{2i} = k_2 \mid C_1^{-i}, C_2^{-i}, \rho) \propto \frac{\rho^{\gamma_1 \gamma_2}}{L_1 L_2} + n_{k_1 k_2}^{-i}. \quad (44)$$

Alternatively, the conditional sampler decomposes the joint distribution of c_{1i} and c_{2i} as

$$\begin{aligned} & \pi(c_{1i} = k_1, c_{2i} = k_2 \mid C_1^{-i}, C_2^{-i}, \rho) \\ &= \pi(c_{2i} = k_2 \mid c_{1i} = k_1, C_1^{-i}, C_2^{-i}, \rho) \pi(c_{1i} = k_1 \mid C_1^{-i}, C_2^{-i}, \rho). \end{aligned} \quad (45)$$

By summing over k_2 in (44), we see that

$$\pi(c_{1i} = k_1 \mid C_1^{-i}, C_2^{-i}, \rho) \propto \frac{\rho^{\gamma_1 \gamma_2}}{L_1} + n_{1k_1}^{-i}, \quad (46)$$

$$\pi(c_{2i} = k_2 \mid c_{1i} = k_1, C_1^{-i}, C_2^{-i}, \rho) \propto \frac{\rho^{\gamma_1 \gamma_2}}{L_1 L_2} + n_{k_1 k_2}^{-i}. \quad (47)$$

Note that the conditional distribution of c_{2i} in (47) only depends on objects with the same value of c_{1i} . When ρ is fixed, we have that

$$\pi(c_{1i} = k_1, c_{2i} = k_2 \mid -) \propto f(X_i; (\theta_{1k_1}^*, \theta_{2k_2}^*)) \left\{ \frac{\rho^{\gamma_1 \gamma_2}}{L_1} + n_{1k_1}^{-i} \right\} \left\{ \frac{\rho^{\gamma_1 \gamma_2}}{L_1 L_2} + n_{k_1 k_2}^{-i} \right\}. \quad (48)$$

Since $f(X_i; (\theta_{1k_1}^*, \theta_{2k_2}^*))$ factorizes into a product, we can use compositional sampling to simulate $\pi(c_{1i} \mid -)$ and then $\pi(c_{2i} \mid c_{1i}, -)$. For the random ρ case, we will need to include the latent probability vectors \tilde{q}_1 and \tilde{q}_2 . In that case, we have that

$$\pi(c_{1i} = k_1, c_{2i} = k_2 \mid C_1^{-i}, C_2^{-i}, \tilde{q}_1, \tilde{q}_2, \rho) \propto \rho \tilde{q}_{1k_1} \tilde{q}_{2k_2} + n_{k_1 k_2}^{-i}, \quad (49)$$

and so

$$\pi(c_{1i} = k_1, c_{2i} = k_2 \mid -) \propto f(X_i; (\theta_{1k_1}^*, \theta_{2k_2}^*)) \left\{ \rho \tilde{q}_{1k_1} + n_{1k_1}^{-i} \right\} \left\{ \rho \tilde{q}_{1k_1} \tilde{q}_{2k_2} + n_{k_1 k_2}^{-i} \right\}. \quad (50)$$

In general, the conditional sampling scheme leads to far better mixing of the partitions than the joint sampling scheme. Observe that the reverse conditional, i.e. doing compositional sampling of c_{2i} then $c_{1i} \mid c_{2i}$, is completely symmetric. Therefore, one can do either conditional sampler in practice, or even alternate between the conditional samplers from iteration to iteration. We have found that either order/alternation leads to similar efficiency, so for our simulations and the application, we implement the scheme outlined above.

When $V \geq 2$, we construct a similar sampler by taking sums across the dimensions of the V -dimensional contingency array. For the uncorrelated views model, the full conditional of the labels for object i is

$$\pi(c_{1i} = k_1, \dots, c_{Vi} = k_V \mid -) \propto \prod_{v=1}^V f_v(X_{vi}; \theta_{vk_v}^*) \times \left\{ \rho \prod_{v=1}^V \tilde{q}_{vk_v} + n_{k_1 \dots k_V}^{-i} \right\}, \quad (51)$$

where $n_{k_1 \dots k_V}^{-i}$ are entries in the contingency array for $C_1^{-i}, \dots, C_V^{-i}$. One conditional sampling scheme is

$$\begin{aligned} & \pi(c_{1i} = k_1, \dots, c_{Vi} = k_V \mid -) \\ & \propto f_1(X_{1i}; \theta_{1i}^*) \left\{ \rho \tilde{q}_{1k_1} + n_{1k_1}^{-i} \right\} \prod_{v=2}^V f_v(X_{vi}; \theta_{vk_v}^*) \left\{ \rho \prod_{u=1}^v \tilde{q}_{uk_u} + n_{k_1 \dots k_u}^{-i} \right\}, \end{aligned} \quad (52)$$

but analogous equations hold for any permutation of $[V]$, e.g., if ω is a permutation of $[V]$, then

$$\begin{aligned} & \pi(c_{\omega(1)i} = k_{\omega(1)}, \dots, c_{\omega(V)i} = k_{\omega(V)} \mid -) \\ & \propto f_{\omega(1)}(X_{\omega(1)i}; \theta_{\omega(1)i}^*) \left\{ \rho \tilde{q}_{\omega(1)k_{\omega(1)}} + n_{\omega(1)k_{\omega(1)}}^{-i} \right\} \end{aligned} \quad (53)$$

$$\times \prod_{v=2}^V f_{\omega(v)}(X_{\omega(v)i}; \theta_{\omega(v)i}^*) \left\{ \rho \prod_{u=1}^v \tilde{q}_{\omega(u)k_{\omega(u)}} + n_{k_{\omega(1)} \dots k_{\omega(u)}}^{-i} \right\}. \quad (54)$$

A similar guarantee holds for the correlated views model.

B.2 ADDITIONAL REMARKS ON TWO UNCORRELATED VIEWS ILLUSTRATION

The dependence between partitions aids inference on C_2 , allowing CLIC to outperform competitors. In addition, samples from $\pi(C_1, C_2 \mid \mathbf{X})$ make it possible to infer the degree of dependence between the partitions. Figures 5 and 6 show the estimated posterior distributions of the TARI for CLIC and the t-HDP under the two different overlaps. In both overlaps, CLIC can model a wide range

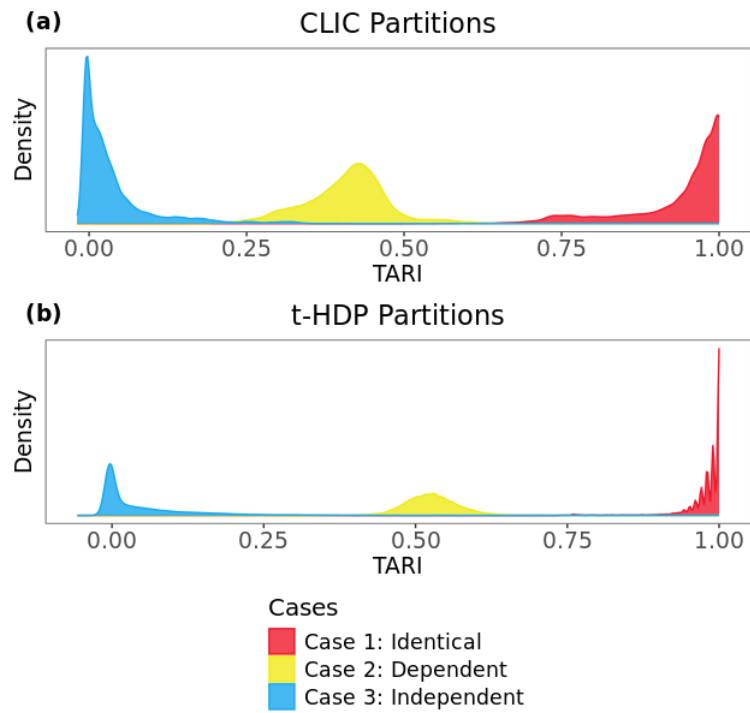


Figure 5: Posterior distributions of the TARI for CLIC and the t-HDP under the first overlap ($\eta^2 = 0.2$).

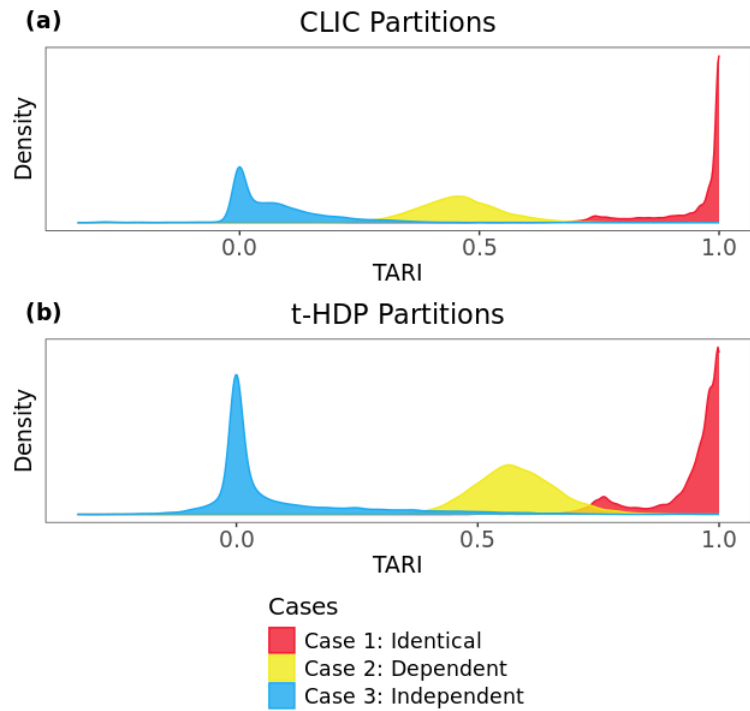


Figure 6: Posterior distributions of the TARI for CLIC and the t-HDP under the second overlap ($\eta^2 = 0.45$).

of dependence structures for random partitions. In cases 1 and 3, the TARI posterior concentrates near 1 and 0, respectively, whereas for case 2, the posterior concentrates between 0.25 and 0.75. We can see similar, but distinct posterior distributions for the t-HDP. For instance, in case 2 under both overlaps, the t-HDP tends to produce clusterings with a higher TARI than those from the CLIC posterior. Hence, while both strategies may lead to similar point estimates, inference on the clustering dependence structure differs between CLIC and the t-HDP. In addition, the computation time for each method is recorded in Table 5.

Overlap	Case	CLIC	t-HDP	EM	IDPs
$\eta^2 = 0.2$	1	31.150	314.780	0.023	28.177
	2	30.105	314.860	0.019	15.681
	3	30.161	316.797	0.022	27.405
$\eta^2 = 0.45$	1	32.512	316.287	0.025	29.427
	2	30.903	314.624	0.034	15.843
	3	29.372	316.704	0.022	27.573

Table 5: Computation time (in seconds) for CLIC and competitors in the two uncorrelated view simulation study, including time to run the MCMC sampler and calculate the point estimate. All Bayesian methods are run for 30,000 iterations. CLIC is substantially more efficient than the t-HDP, though the EM algorithm is the fastest option.

B.3 ILLUSTRATION WITH TWO CORRELATED VIEWS

We simulate the data with $(X_i | c_{1i}, c_{2i}) \sim \mathcal{N}(X_{1i}; \{-1\}^{c_{1i}+1}, 0.2) \times \mathcal{N}(X_{2i}; \{-1\}^{c_{2i}} X_{1i}, \eta^2)$, where η^2 takes the same values as in the uncorrelated setting in Section 5. If $c_{2i} = 1$ observation i has a negative relationship with the covariates, while if $c_{2i} = 2$ they have a positive association. Figure 7 shows the true values for C_1 and C_2 along with the synthetic data. For the PCDP, we assume $\pi(X_i; \theta_i) = \mathcal{N}(X_{1i}; \theta_{1i}, \sigma_1^2) \times \mathcal{N}(X_{2i}; \theta_{2i} X_{1i}, \sigma_2^2)$ and $H_v(\theta) = \mathcal{N}(\theta; \mu_0, \sigma_0^2)$. We compare CLIC with a correlated implementation of the t-HDP (which we call the ct-HDP), two IDPs where one DP clusters \mathbf{X}_1 and the other clusters $\mathbf{X}_2 | \mathbf{X}_1$ using a mixture of linear regressions, and the EM algorithm applied to \mathbf{X}_1 and a linear regression implementation of the EM algorithm (Leisch, 2004) applied to $\mathbf{X}_2 | \mathbf{X}_1$. For both CLIC and the IDPs, the point estimates are obtained by minimizing the VI loss.

The corresponding ARIs are given in Table 6. CLIC coherently clusters the two views and attains high ARI values in all three cases. In case 1, the outcome can be predicted by first partitioning the covariates and then fitting a regression model within each cluster. CLIC and the ct-HDP are able to identify and exploit this relationship, leading to ARIs of 0.941 and 0.960, respectively, greatly

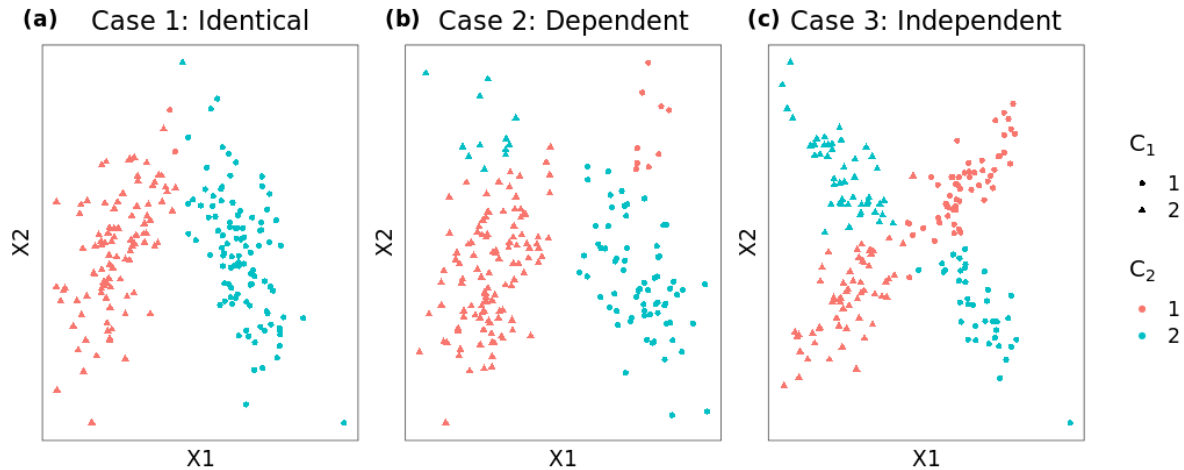


Figure 7: The synthetic data simulated in the correlated views setting, where shapes and colors correspond to the true values of C_1 and C_2 . Here, we have that C_2 clusters are characterized by differing regression slopes.

	CLIC	ct-HDP	IDPs	EM
Case 1	(0.941, 0.941)	(0.960, 0.960)	(0.941, 0.531)	(0.941, 0.606)
Case 2	(1.000, 0.775)	(1.000, 0.775)	(1.000, 0.704)	(1.000, 0.721)
Case 3	(0.921, 0.883)	(0.921, 0.883)	(0.921, 0.883)	(0.921, 0.883)

Table 6: The adjusted Rand indices (ARI) between the true (C_1, C_2) and the point estimates computed by CLIC, the ct-HDP, two IDPs (where the second model uses profile regression of \mathbf{X}_2 on \mathbf{X}_1), and independent EM for the synthetic data. CLIC has the joint highest accuracy for estimating (C_1, C_2) with the exception of case 1, where the ct-HDP correctly classifies one extra object than CLIC.

outperforming IDPs and EM. This task becomes far more difficult in case 2, where objects in either of the true clusters in C_1 can have positive or negative correlation between X_{1i} and X_{2i} . However, objects in cluster 1 of C_1 are more likely to have a positive association, and objects in cluster 2 of C_1 tend to have a negative relationship. All methods find this regime challenging, in part because the separation between the C_1 clusters leads to wide gaps in the regression lines. However, CLIC and the ct-HDP still outperform IDPs and EM in classifying the objects because they account for clustering dependence. In case 3, objects in either cluster of C_1 are equally likely to have positive or negative correlation. Due to the separation between the clusters, all four methods return the same point estimate and achieve high ARI values with the true partitions. A comparison between the posterior distributions of the TARI under CLIC and the t-HDP is given in Figure 8. As in the uncorrelated views setting, the posterior for the TARI in case 1 is more diffuse for the t-HDP, and the posterior for case 3 is more concentrated at 0 for CLIC.

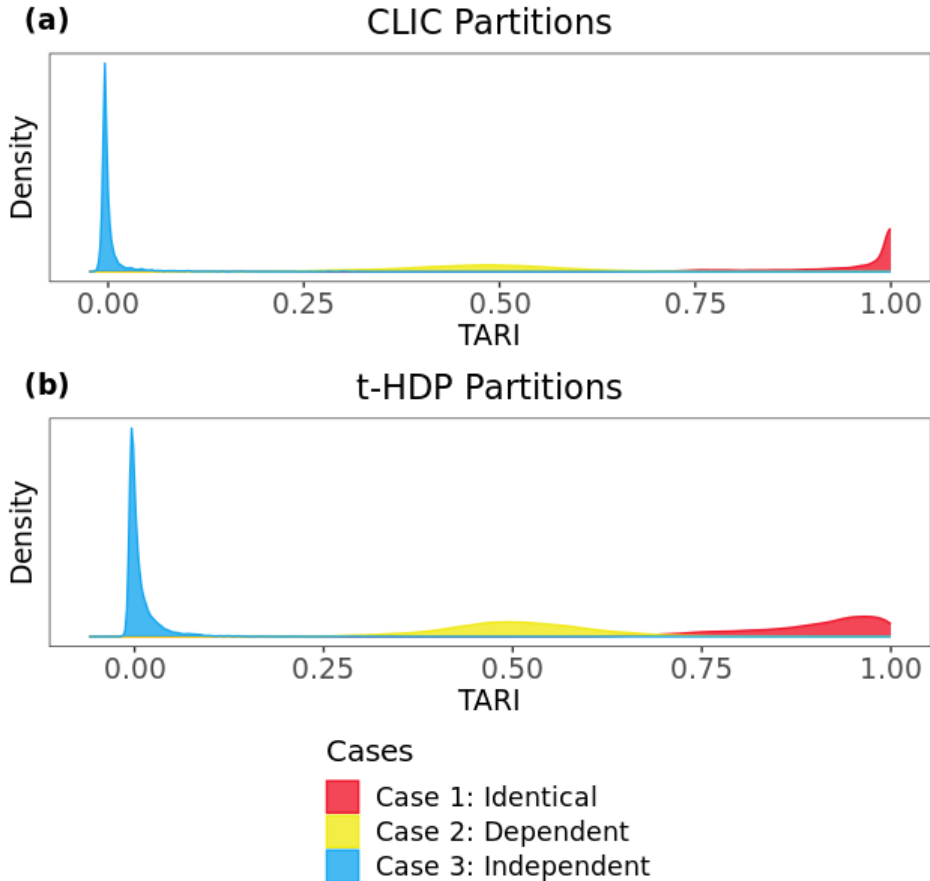


Figure 8: Estimated posterior distributions of the TARI under two correlated views for CLIC and the t-HDP based on synthetic data.

B.4 ADDITIONAL REMARKS ON THREE VIEWS SETTING

The computation times for CLIC, the t-HDP, EM, and the IDPs were 60.029, 518.545, 0.033, and 23.477 seconds respectively, where each Bayesian algorithm is run for 30,000 iterations.

B.5 ADDITIONAL REMARKS ON VARYING DIMENSION AND SAMPLE SIZE SIMULATIONS

All Bayesian methods are ran for 30,000 iterations with 5,000 as warm-up, and every other iteration was thinned. Computation times for all methods are displayed in Table 7. The PCDP uses base measures $H_v(\theta) = \mathcal{N}_{d_v}(\theta; \mathbf{0}_{d_v}, I_{d_v})$, where $\mathbf{0}_{d_v}$ and I_{d_v} are the d_v -dimensional zero vector and identity matrix. We also set $\gamma_1 = \gamma_2 = 1$, $L_1 = L_2 = 10$, and $1/\sigma_v^2 \sim \text{Gamma}(1, 1)$. For the t-HDP, we use the function `telescopic_HDP_NNIW_multi.R` from the [Github repository](#) for the method. We use the default hyperparameters $H_0 = H = 10$, concentration parameters equal to 0.1, and Normal-inverse-Wishart scale equal to 0.1. Like the PCDP, the IDPs and DP also have standard Gaussian base

$n = 100$					
d_2	CLIC	t-HDP	EM	IDPs	DP
2	16.960	11875.856	0.960	11.106	6.343
10	18.685	14577.428	0.926	12.774	8.040
25	22.918	16182.596	1.235	16.564	11.883
$n = 200$					
d_2	CLIC	t-HDP	EM	IDPs	DP
2	62.835	17647.145	3.139	29.664	16.702
10	66.319	21457.653	3.004	33.316	19.830
25	73.641	23917.661	2.041	40.047	26.918
$n = 500$					
d_2	CLIC	t-HDP	EM	IDPs	DP
2	294.488	34363.581	10.147	136.790	81.237
10	300.070	41564.017	11.273	147.140	80.839
25	317.207	46181.697	39.278	161.755	96.035

Table 7: Computation time (in seconds) for all methods to compute the point estimates along both views.

measures, 10 components, and a variance prior set to a Gamma(1, 1) distribution. The EM algorithm is implemented in the same manner as the other simulations.

B.6 MIXING AND CONVERGENCE FOR THE TWO VIEWS SETTING

Overlap	Case 1	Case 2	Case 3
$\eta^2 = 0.2$	480.852	598.751	378.956
$\eta^2 = 0.45$	366.986	919.625	219.241

Table 8: Effective sample size of $R(C_1, C_2)$ for each case and overlap in the two uncorrelated views setting.

We find that the mixing for the partitions is much better when ρ is given a hyperprior and updated during the MCMC sampler than when it is fixed. In the main article, we present two alternative priors and corresponding sampling strategies for updating ρ . The first is to use a gamma prior as in [Escobar and West \(1995\)](#), which is semiconjugate. The second is to use a griddy-Gibbs sampler ([Ritter and Tanner, 1992](#)) and allow ρ to vary across a pre-specified grid. In the simulations, we assume that $\rho \sim \text{Gamma}(1, 1)$ and fix $\gamma_1 = \gamma_2 = \gamma = 1$.

Recall that $0 \leq R(C_1, C_2) \leq 1$. Trace plots for $R(C_1, C_2)$ are given in [Figures 9](#) (for uncorrelated views) and [10](#) (for correlated views). Additionally, the effective sample sizes for the uncorrelated views

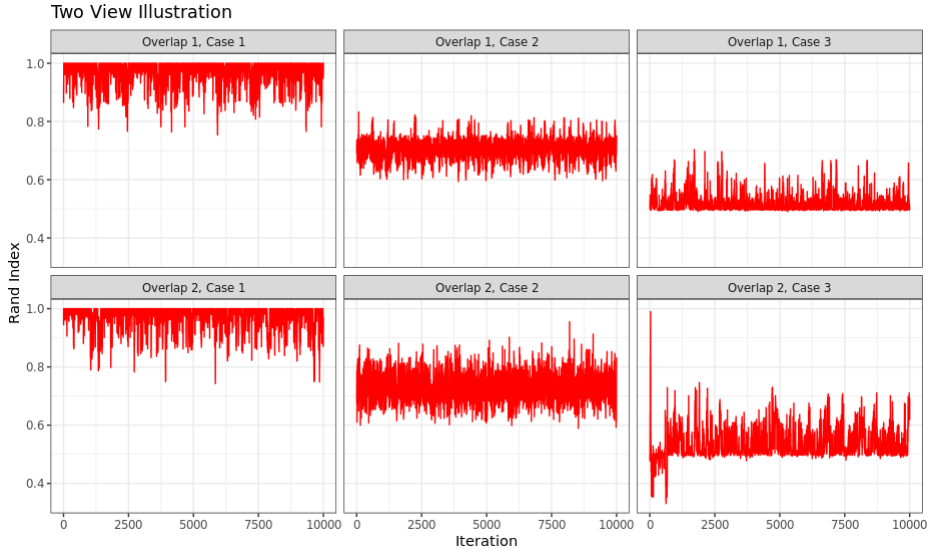


Figure 9: Traceplots for $R(C_1, C_2)$ for each case and overlap (i.e., value of η^2) in the two view setting. The Rand index may mix worse when it hits either its upper or lower boundary, and mixes better when it is in $(0, 1)$.

simulations are in Table 8, and for the correlated views simulations these values are 558.467 (case 1), 678.036 (case 2), and 335.535 (case 3). Convergence of the Rand index in all simulations is rapid, but the Gibbs sampler is most efficient when the true partitions are weakly dependent (i.e., case 2). Efficiency can decrease when the true partitions exhibit either case 1 or case 3. In case 1, the true Rand index is equal to 1, and so samples of $R(C_1, C_2)$ tend to accumulate near its upper bound, which results in worse mixing than the weak dependence case. While $R(C_1, C_2)$ is bounded below by 0, we show in Theorem 3 that $\mathbb{E}[R(C_1, C_2)] = \tau_{12} \geq (1 + \gamma^2)/(1 + \gamma)^2 = 1/2$. Though there is still positive posterior probability that $R(C_1, C_2) < 1/2$, the vast majority of samples from the Rand index are at least as large as $1/2$. Hence, in case 3, samples of $R(C_1, C_2)$ accumulate near an (approximate) lower bound, resulting in correlated draws.

B.7 MIXING AND CONVERGENCE FOR THE THREE VIEWS SETTING

Traceplots for the pairwise Rand indices are given in Figure 11. The effective sample size is 465.9618 for $R(C_1, C_2)$, 565.8382 for $R(C_1, C_3)$, and 365.5251 for $R(C_2, C_3)$, similar to the mixing we observe in the two view case.

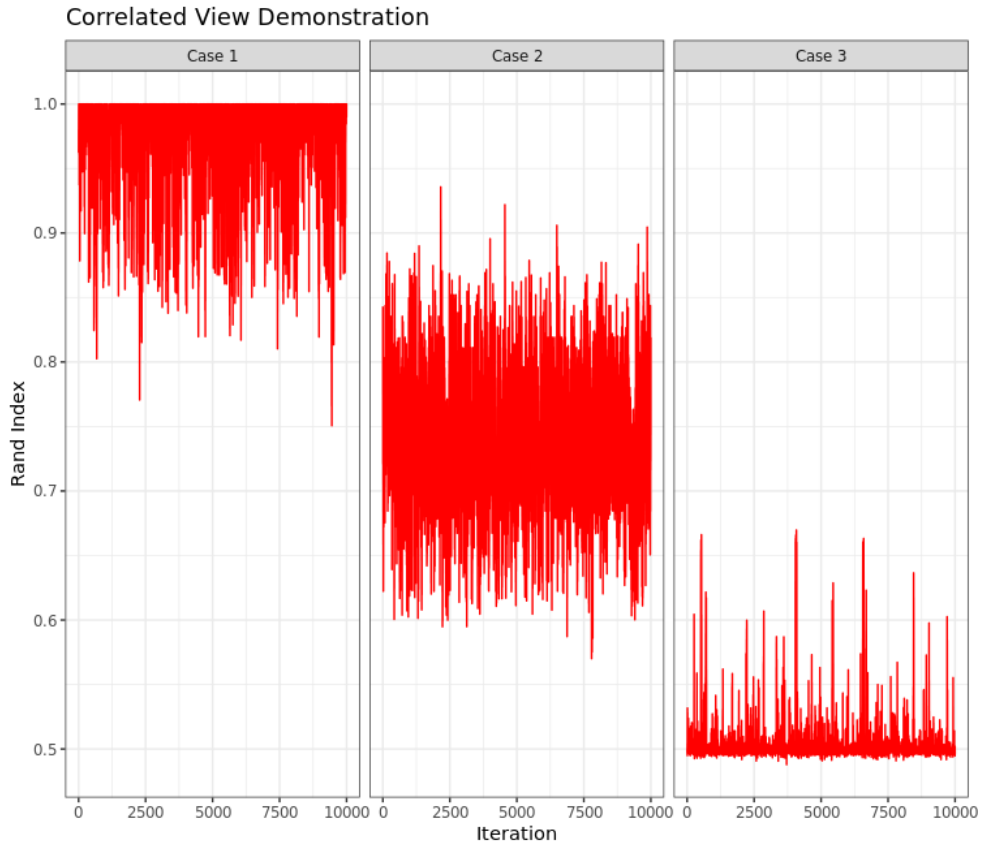


Figure 10: Traceplots for $R(C_1, C_2)$ in the illustration discussed in Section B.3.

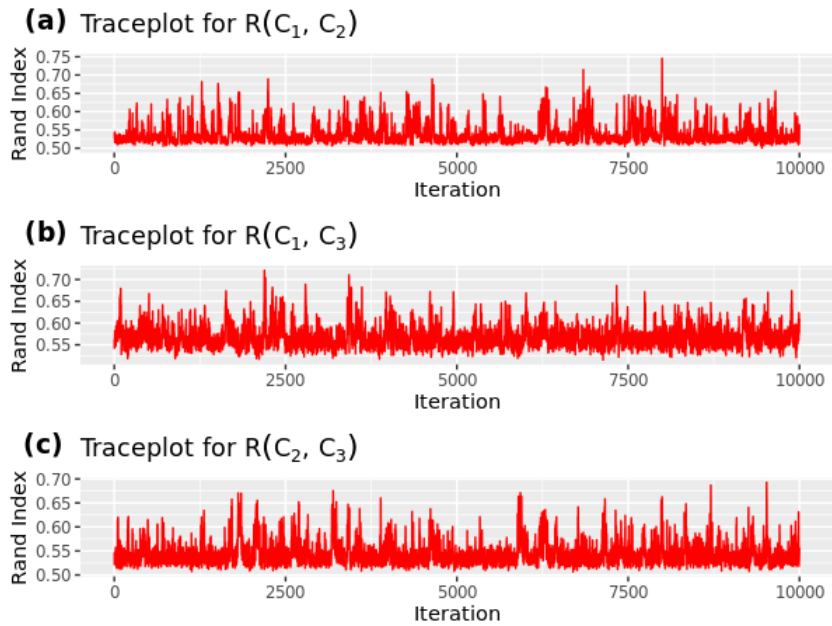


Figure 11: Traceplots for the all pairwise Rand indices for the three partitions in the three view setting.

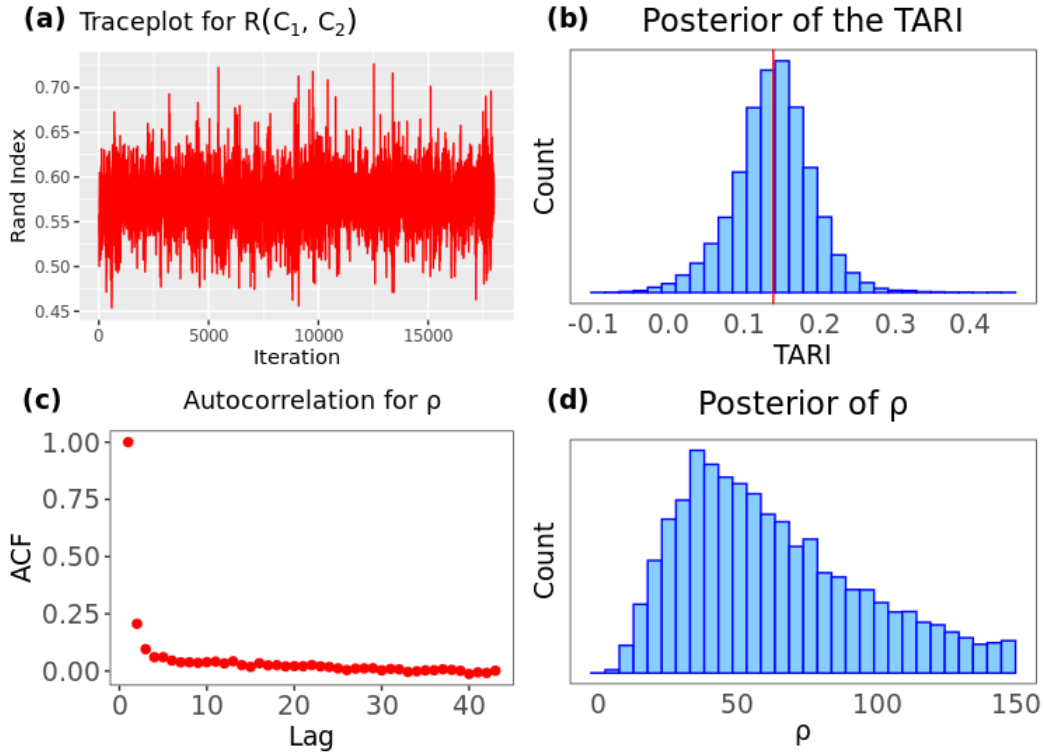


Figure 12: MCMC diagnostics for the application of CLIC to the Longnecker et al. (2001) data.

C ADDITIONAL DETAILS ON THE CPP APPLICATION

The Longnecker et al. (2001) dataset has $d = 494$ features measured on 2,379 mothers (and their children). First, we subset the data to have gestational age strictly less than 42 weeks in order to remove outliers. Then, we take a random sample of size $n = 1,000$ to help with visualization of the results and to add more uncertainty into the cluster-specific parameters, ultimately making the problem more challenging. Both gestational age and birthweight are normalized to have zero mean and unit standard deviation.

As mentioned in the main article, mixing can improve by using a griddy-Gibbs sampler for ρ . We implement the griddy-Gibbs sampler in the application to the Longnecker et al. (2001) dataset, where ρ has support on a grid from 10^{-2} to 150 in intervals of length 0.5. Figure 12 shows the MCMC diagnostic plots for $R(C_1, C_2)$ and ρ over the 18,000 iterations we use. As we observed in simulations, draws in the Gibbs sampler tend to be more correlated for very low values of the Rand index. The effective sample size of $R(C_1, C_2)$ is 1497.218 and for ρ it is 6251.118. The time it takes to run the MCMC sampler, compute the point estimates, and sample from the posterior of $R(C_1, C_2)$ was 1,592.387 seconds.

D TESTING THE UNCORRELATED AND CORRELATED MODELS

In some applications, it may be of interest to test the two multiview models presented in Section 2. In one model, the views are correlated conditional on the cluster labels, and in the other, the views are uncorrelated. One possibility is to compute the Bayes factor (BF) (Kass and Raftery, 1995) for testing $H_0 : f(X_i; \theta_i) = f_1(X_{1i}; \theta_{1i}) \times f_2(X_{2i}; \theta_{2i})$ vs. $H_1 : f(X_i; \theta_i) = f_1(X_{1i}; \theta_{1i}) \times f_2(X_{2i}; X_{1i}, \theta_{2i})$, which involves computing the marginal likelihood of both models. In many cases, computing the marginal likelihood may be infeasible. An alternate strategy is to specify a variable selection prior for the base measure in the second view. As a simple example, suppose we have $d_2 = 1$ and set $f_1(X_{1i}; \theta_{1i}) = \mathcal{N}(X_{1i}; \theta_{1i}, \Sigma_1)$. For the outcome, say we set $\theta_{2i} = (\alpha_{2i}, \beta_{2i})$ and $f_2(X_{2i}; X_{1i}, \theta_{2i}) = \mathcal{N}(X_{2i}; \alpha_{2i} + X_{1i}^T \beta_{2i}, \sigma_2^2)$. To complete the specification, we take the base measure in the second view to be

$$H_2(\theta_{2k_2}^*) = \mathcal{N}(\alpha_{2k_2}^*; \mu_\alpha, \Sigma_\alpha) \times \{ \lambda \delta_0(\beta_{2k_2}^*) + (1 - \lambda) \mathcal{N}(\beta_{2k_2}^*; \mu_\beta, \Sigma_\beta) \},$$

where $\lambda \in (0, 1)$ and δ_0 is a point-mass at the zero vector. The choice of measure for $\beta_{2k_2}^*$ is a version of the spike-and-slab prior for linear regression models (Mitchell and Beauchamp, 1988; Ishwaran and Rao, 2005). This is equivalent to mixing over a latent variable $\phi \in \{0, 1\}$, where $(\beta_{2k_2}^* | \phi = 1) \sim \delta_0$, $(\beta_{2k_2}^* | \phi = 0) \sim \mathcal{N}(\mu_\beta, \Sigma_\beta)$, and $\pi(\phi = 1 | \lambda) = \lambda$. When $\phi = 1$, model (5) holds, otherwise, model (6) holds. Suppose further that we set $\lambda \sim \text{Beta}(a_\lambda, b_\lambda)$. We could test model (5) against model (6) by calculating the BF of $H_0 : \phi = 1$, or simply $\pi(\phi = 1 | \mathbf{X})$. This could be accomplished using the output of the Gibbs sampler in Section 4 by saving samples $\phi^{(t)}$ for $t = 1, \dots, T$, then applying the approximation $\pi(\phi = 1 | \mathbf{X}) \approx (1/T) \sum_{t=1}^T \mathbf{1}_{\phi^{(t)}=1}$.

E ALTERNATE METHODS OF COMPUTATION

In Section 3, we use a result on HDPs from Camerlenghi et al. (2018) to derive the MEPPF for the cross-partition. As with HDPs, the inclusion of \tilde{q}_1 and \tilde{q}_2 in the Gibbs sampler can be inefficient. However, Theorem 2 shows that we can marginalize out \tilde{q}_1, \tilde{q}_2 from our sampler. As in Section 4, we need to sample from the full conditional distributions of ρ, \mathbf{r}, C_1 , and C_2 , as well as the cluster-specific parameters. Note that

$$\pi(C_1, C_2, \mathbf{r} | \rho, \gamma_1, \gamma_2) = \frac{\gamma_1^{K_1} \gamma_2^{K_2}}{(\rho)^{(n)}} \rho^r \left\{ \prod_{v=1}^2 \frac{\prod_{k_v} (r_{vk_v} - 1)!}{(\gamma_v)^{(|r_v|)}} \right\} \prod_{k_1, k_2} |s(n_{k_1 k_2}, r_{k_1 k_2})|. \quad (55)$$

As before, we have that $\pi(\rho \mid -) \propto \rho^r / (\rho)^{(n)} \pi(\rho)$. The main difficulty is simulating from $\pi(\mathbf{r} \mid -) \propto \pi(C_1, C_2, \mathbf{r} \mid \rho, \gamma_1, \gamma_2)$. Recall that $\pi(\mathbf{r})$ can be simulated by first sampling r from $\pi(r = w \mid \rho) \propto \rho^w$, then generating the root partitions T_1 and T_2 from independent CRP(γ_v) distributions with r customers and taking \mathbf{r} to be their contingency table. Therefore, one possible strategy is to take $\pi(\mathbf{r})$ to be a proposal distribution and to perform a Metropolis-Hastings step within the Gibbs sampler. However, when sampling (T_1, T_2) conditional on (C_1, C_2) , we have to make sure that the number of clusters in T_v is equal to K_v . If the number of clusters in either root partition is not equal to the number of clusters in C_v , the candidate would automatically be rejected. Therefore, one needs to be careful for the proposal distribution of \mathbf{r} in order to preserve the number of clusters. Alternatively, existing samplers for the HDP could be augmented for PCDP, see [Das et al. \(2024\)](#) and references therein for a comprehensive overview.